ANALYTICAL EVALUATION OF THE EFFECTS
OF HEAT TRANSFER AND SKIN FRICTION ON THE
EFFICIENCY OF THE EXPANSION OF A GAS HAVING
A PRANDTL NUMBER OF ONE THROUGH A
CONVERGING - DIVERGING NOZZLE OF
LARGE RADIUS WITH CONSTANT
TEMPERATURE WALLS

Thesis for the Degree of Ph. D.
MICHIGAN STATE UNIVERSITY
Richard Lee Ditsworth

1958

This is to certify that the

thesis entitled

ANALYTICAL EVALUATION OF THE EFFECTS OF HEAT TRANSFER AND
SKIN FRICTION ON THE EFFICIENCY OF THE EXPANSION OF A GAS
HAVING A PRANDTL NUMBER OF ONE THROUGH A CONVERGING-
DIVERGING NOZZLE OF LARGE RADIUS WITH CONSTANT TEMPERATURE
WALLS.

presented by

RICHARD L. DITSWORTH

**has been accepted towards fulfillment
of the requirements for**

Doctor of Philosophy degree in Mechanical Engineering

Major professor

Date August 22, 1958

O-169

ANALYTICAL EVALUATION OF THE EFFECTS OF HEAT TRANSFER
AND SKIN FRICTION ON THE EFFICIENCY OF THE EXPANSION
OF A GAS HAVING A PRANDTL NUMBER OF ONE THROUGH A
CONVERGING-DIVERGING NOZZLE OF LARGE RADIUS WITH
CONSTANT TEMPERATURE WALLS
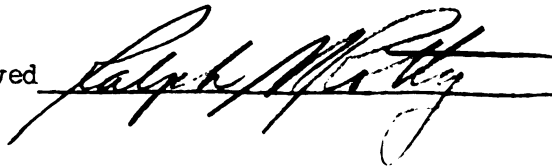
By

Richard Lee Ditsworth

AN ABSTRACT

Submitted to the School for Advanced Graduate Studies of
Michigan State University of Agriculture and
Applied Science in partial fulfillment of
the requirements for the degree of

DOCTOR OF PHILOSOPHY

Department of Mechanical Engineering

1958

Approved _Ralph M_____

Richard Lee Ditsworth

AN ABSTRACT

The effects of skin friction and heat transfer were evaluated for
a gas expanding through a nozzle. This study was limited to viscous
and compressible gases with Prandtl number of unity. The nozzle size
was taken to be sufficiently large so that boundary layer thicknesses
could be neglected, the nozzle was conically-shaped in both converging
and diverging sections, and the nozzle walls were assumed to have a
constant temperature.

The evaluation of effects on exit Mach number were obtained using
a generalized one-dimensional approach. The skin friction and heat
transfer were established from three-dimensional considerations
(axially-symmetric flow). This required consideration of velocity and
temperature gradients occurring in a boundary layer between the wall
and the main potential flow. Laminar boundary layer differential
equations for continuity, energy and momentum were taken as the basis
for boundary layer analysis. A series of transformations, due to
Mangler and to Stewartson, were used to reduce equations from a three-
dimensional compressible case to a form similar to a two-dimensional
and essentially incompressible case. An additional transformation,
including an exponential velocity distribution for the potential flow,
was used to obtain a set of ordinary differential equations of the
same form previously solved and tabulated in NACA Report 1293 by Cohen
and Reshotko.

In order to utilize the temperature and velocity gradient information from boundary layer considerations, expressions were developed in a generalized one-dimensional coordinate system. Solution of these expressions gave the effects of skin friction and heat transfer on nozzle efficiency.

Nozzle efficiencies were given in graphical form as a function of a parameter dependent on initial conditions. From these results of the analysis, the following conclusions were reached:

1. Heat transfer effects were dominant in the converging section, and this dominance may extend slightly into the diverging region for much colder walls.

2. Skin friction effects become more important in the diverging section.

3. Combined effects influence reduction in efficiency of a Mach 3.0 nozzle of the order of 0.2 per cent.

4. The effect of the boundary layer thickness on flow area, though small for nozzles of large radius, should be considered along with skin friction and heat transfer effects to improve reliability of nozzle efficiency predictions.

ANALYTICAL EVALUATION OF THE EFFECTS OF HEAT TRANSFER
AND SKIN FRICTION ON THE EFFICIENCY OF THE EXPANSION
OF A GAS HAVING A PRANDTL NUMBER OF ONE THROUGH A
CONVERGING-DIVERGING NOZZLE OF LARGE RADIUS WITH
CONSTANT TEMPERATURE WALLS

By

Richard Lee Ditsworth

A THESIS

Submitted to the School for Advanced Graduate Studies of
Michigan State University of Agriculture and
Applied Science in partial fulfillment of
the requirements for the degree of

DOCTOR OF PHILOSOPHY

Department of Mechanical Engineering

1958

ACKNOWLEDGEMENT

VITA

Richard Lee Ditsworth

candidate for the degree of

Doctor of Philosophy

Final examination, August 22, 1958, 10:15 A.M., Room 113,
Olds Hall

Dissertation: Analytical Evaluation of the Effects of Heat
              Transfer and Skin Friction on the Efficiency of
              the Expansion of a Gas Having a Prandtl Number
              of One Through a Converging-Diverging Nozzle of
              Large Radius with Constant Temperature Walls

Outline of Studies

    Major Subject: Mechanical Engineering
    Minor Subjects: Mathematics, Physics

Biographical Items

    Born: April 15, 1925, Algona, Iowa
    Undergraduate Studies: Iowa State College, 1942-43;
        cont. 1946-49
    Graduate Studies: Iowa State College 1951-52; Michigan
        State University, 1953-58

Experience: Navigator, Army Air Corp, 1943-46; Engineer,
            Chance Vought Aircraft, 1949-51; Instructor in
            Applied Mechanics, Iowa State College, 1952-53;
            Instructor in Mechanical Engineering, Michigan
            State University, 1953-58

Member of Phi Kappa Phi, Sigma Xi, Pi Tau Sigma, Sigma Pi Sigma

TABLE OF CONTENTS

LIST OF FIGURES

LIST OF TABLES

NOMENCLATURE

Symbols used:

A   cross section area

α sonic velocity, $(= \gamma \bar{R} T)$

C_1, c_1 arbitrary constants

c_f local skin friction coefficient (See Eq. (87))

c_p specific heat at constant pressure $\left(= \dfrac{\gamma \bar{R}}{\gamma - 1}\right)$

c_v specific heat at constant volume

Eff_{nA} nozzle efficiency based on same exit area

Eff_{nP} nozzle efficiency based on same exit pressure

F   force

$f(\eta)$ function of variable η related to stream function $\left(= \psi'' \sqrt{\dfrac{K_1}{2 u_e'' \, \nu_o L}}\right)$

h   enthalpy per unit mass

h_{st} boundary layer stagnation enthalpy $\left(= c_p T + \dfrac{u^2}{2}\right)$

K_1 constant in velocity distribution (See Eq. (78))

k   thermal conductivity

k_{su} Sutherlands constant

L   arbitrary length

L_1 length of convergent section (See Fig. 1)

L_2 length of divergent section (See Fig. 1)

M Mach number $\left(= \dfrac{u}{\alpha} \right)$

m constant exponent in velocity distribution (See Eq. (69))

Pr Prandtl number $\left(= \dfrac{c_p \mu}{k} \right)$

p static pressure

q_r, q_z velocity in cylindrical coordinate system

Q heat energy transfer

q_w rate of heat transfer at wall

r cylindrical coordinate – radial length

R nozzle radius

$\bar{R}$ specific gas constant

R_e Reynolds number $\left(= \dfrac{u\,x}{\nu} \right)$

S enthalpy function $\left(= \dfrac{h_{st}}{h_0} - 1 \right)$

T static temperature

u longitudinal velocity component

V velocity in one dimensional system

v normal velocity component

w mass flow rate

x length coordinate along wall (See Fig. 1)

x' first transformed length coordinate (See Eq. (53))

x'' second transformed length coordinate (See Eq. (59))

y normal length coordinate (See Fig. 1)

y' first transformed normal length coordinate (See Eq. (54))

y''	second transformed normal length coordinate (See Eq. (60))	
z	axial coordinate of nozzle	
α	sonic velocity	$\left(= \sqrt{\gamma \bar{R} T}\right)$
β	constant in Eq. (73)	$\left(= \dfrac{2m}{m + 1}\right)$
γ	ratio of specific heats	$\left(= \dfrac{c_p}{c_v}\right)$
δ	thickness of boundary layer	
Δ	parameter of initial conditions (See Eq. (112))	
Δ	small interval	
η	variable (See Eq. (79))	
ϑ	nozzle wall angles (See Fig. 1)	
λ	viscosity proportionality constant (See Eq. (62))	
μ	dynamic viscosity	
ν	kinematic viscosity (μ/ρ)	
ρ	mass density	
ρu	mass velocity	
τ	shear stress (See Eq. (88))	
ψ	stream function	

Subscripts used:

e	local flow outside boundary layer
min	minimum
p	polar coordinates
r	radial direction
S	isentropic process
SA	isentropic process based on same area

SP	isentropic process based on same pressure
St	stagnation values
z	axial direction
w	wall value
*	conditions where $M = 1$
o	stagnation value. In boundary layer equations, refers to free stream stagnation value
1	converging section
2	diverging section
'	single prime refers to first transformed coordinates
"	double prime refers to second transformed coordinates
$x = 0$	origin of coordinate system (x, y)

Others:

$\underline{V}$	sub bar means vector quantity
[o]	order of magnitude of
$\cong$	approximately equal to
$(\overline{})$	average quantity for given interval

INTRODUCTION

The purpose of a nozzle is to control the expansion of a fluid to a lower pressure region in order to obtain a high velocity. If the medium is a compressible fluid, it is possible for acceleration from subsonic to supersonic speeds to occur if the nozzle has a convergent section followed by one that is divergent. In such a case the speed at the minimum cross section or throat is identical to the speed of sound for the state of the medium at the throat and the Mach number is equal to one.

From an idealized thermodynamic standpoint, the expansion of a gas through a nozzle is regarded as occurring without friction or transfer of heat, and is described as a reversible and adiabatic process. Hence, using the assumption of an isentropic process, an ideal exit velocity may be calculated when the state of the upstream gas and the exhaust region pressure is given. Since the actual velocities obtained for the same operating conditions vary somewhat from the ideal, the engineer uses a factor relating the above two velocities. In many applications, performance evaluated in this manner is sufficiently accurate, especially when there is an abundance of empirical test data for accepted nozzle shapes and sizes tested at different pressure ratios and essentially adiabatic conditions.

In the case of an exhaust nozzle for a jet engine, the situation is somewhat different. The size is necessarily large, and the upstream temperature is high. The thrust performance, resulting from the

change of the momentum of the gas, is particularly dependent on an accurate measure of the efficiency of the nozzle and a difference of one per cent or less may mean the difference between success or failure. If the inlet temperature is in the order of 3600°R, the external walls of the nozzle must be cooled, and hence the effects of heat transferred should be considered. Since throat diameters are large, perhaps one to two feet, the difficulties of obtaining reliable experimental information is magnified and an analytical evaluation of such losses as those due to friction and heat transfer at the wall occurring as a viscous compressible fluid expands to supersonic speeds, has increased value.

THEORETICAL ANALYSIS

Objectives

The purpose of this investigation was twofold: first, to evaluate
quantitatively the relative magnitude of skin friction and heat losses
in a viscous compressible fluid expanding to supersonic speed through a
nozzle with straight walls at a constant temperature; and second, to
evaluate the effects of skin friction and heat losses on the exit vel-
ocity of the fluid. In addition to providing a better understanding
of flow phenomena, the information could be used to establish theoret-
ical maximums in nozzle efficiency coefficients. Not all of the causes
of change from ideal performance by an actual gas have been considered:
variation of specific heats, displacement thickness of boundary layer,
turbulence, and dissociation are some factors which have been omitted
in this study.

Assumptions

A converging-diverging nozzle was considered as follows:

1. The walls were conical with the converging section slightly
   rounded at the throat, as shown in Fig. 1.

2. The radius was considered as being large, e.g., a throat
   diameter of at least six inches.

3. The wall surface was smooth
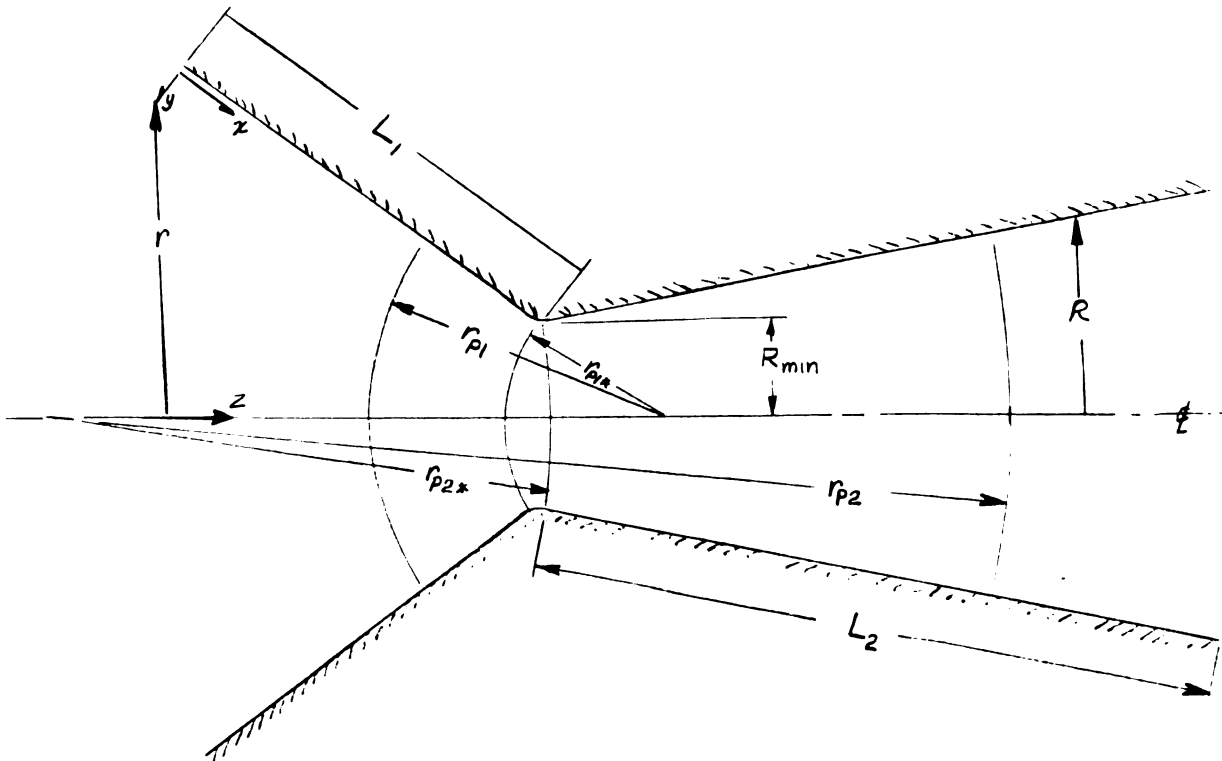
Fig. 1. Converging-diverging nozzle with space coordinates
         and their origins.

The system undergoing the expansion process was assumed to be
a compressible pure substance with these properties:

1. The applicable equation of state was $p = \rho \bar{R} T$.

2. Specific heat values were constant.

3. Viscosity was dependent on temperature only, and suitably
   described by the Sutherland formula.

4. The value of Prandtl number ($\frac{C_p \mu}{k}$) was unity.

5. The ratio of specific heats (γ) was equal to 7/5 for
   purposes of obtaining numerical results.

6. No phase change occurred.

The flow phenomena resulting in supersonic speeds in the gas in
the absence of body forces, was considered from two points of view.
The first was that of a steady and continuous one-dimensional flow
occurring with surface forces or wall friction and external heat trans-
fer. The term "one-dimensional" means the fluid properties and vel-
ocity are constant over each cross section. Thermodynamic and fluid
dynamic reasoning may be utilized to obtain mathematical expressions
which include terms for skin friction and heat transfer. In order to
solve these differential equations and evaluate the state and velocity
of the fluid at the exit section, additional information was needed
concerning the skin friction and heat transfer terms. This information
is the velocity and temperature gradients in the fluid at the wall.
This required consideration of the flow immediate to the solid boundary,
and hence the second point of view. It is generally accepted that flow
in a channel or around a body may be considered as consisting of a thin
layer of fluid next to the wall, where viscous and inertia terms in the

equation of motion are taken as having the same order of magnitude, and the main body or "core" of fluid with negligible viscous forces and heat transfer located external to the boundary layer. Analysis of an axial-symmetric boundary layer with large external axial pressure gradients and heat transfer at the wall was necessary to obtain the desired gradients of velocity and temperature at the wall.

Assumptions for the generalized one-dimensional flow were as follows:

1. The process was steady and continuous.

2. The velocity, pressure, and temperature are uniform at any given cross section.

3. A frictional shearing stress and heat transfer occur at the nozzle wall area.

Assumptions made for the "core", or potential flow external to the boundary layer were:

1. The process was frictionless, adiabatic, steady, and continuous.

2. An apparent sink-source type flow was taken to describe the mass velocity ($\rho\, u_e$) distribution in the converging and diverging sections respectively, with uniform properties at any given r_p , except in the region close to the throat.

3. The potential flow does not depend on the boundary layer flow in regard to first order effects.

The considerations for the boundary layer flow were:

1. The flow was assumed to be laminar. This was reasonable in view of the large negative pressure gradient existing

in the potential flow, a favorable condition to forestall
a transition to turbulent flow. Further, it has been
found by Lees[1] that cooling the fluid noticeably increases
the stability of the laminar layer.

2. The usual boundary layer assumptions for laminar flow were
taken; that is, the large velocity change from wall to the
potential flow occurred in a very thin layer, δ , and
inertia and viscous stresses were of the same order of
magnitude.

In all cases the flow phenomena must behave according to the fol-
lowing basic physical laws:

1. Equation of state.

2. Continuity equation.

3. Energy equation.

4. Momentum equation.

_____

[1]Lees, L. The Stability of the Laminar Boundary Layer in a
Compressible Fluid. NACA Tech. Note, No. 1360, 1947.

Mathematical Development

Generalized One-dimensional Flow

A control volume analysis is used to obtain the one-dimensional expressions that are needed. The control surface is shown in Fig. 2.
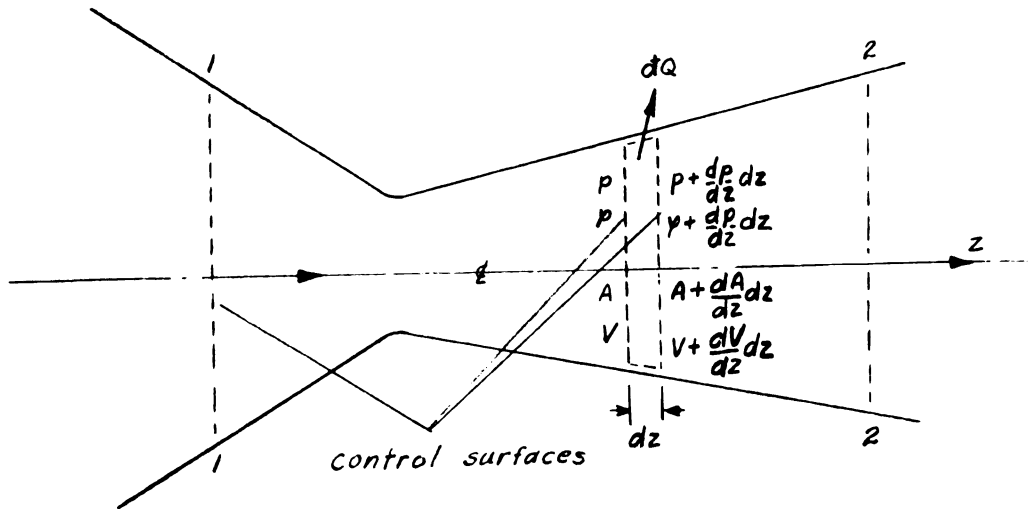
Fig. 2. Control Surfaces

A basic expression of continuity for steady flow is in the form of a surface integral:

$$\oint \rho \underline{V} \cdot d\underline{A} = 0 \tag{1}$$

and when integrated for constant ρ and V at each cross section, one obtains:

$$w = \rho_1 V_1 A_1 = \rho_2 V_2 A_2 \qquad (2)$$

or in logarithmic differential form:

$$0 = \frac{dw}{w} = \frac{d\rho}{\rho} + \frac{dV}{V} + \frac{dA}{A} \qquad (3)$$

In the absence of shear work and with negligible body forces, the First Law of Thermodynamics for steady flow may be written:

$$w(h_1 + \frac{V_1^2}{2}) + w Q = w(h + \frac{V^2}{2}) \qquad (4)$$

or, considering the changes occurring through a distance dz , the energy equation is:

$$wdQ = w\left(dh + \frac{dV^2}{2}\right) \qquad (5)$$

The definition of constant pressure specific heat:

$$c_p = \frac{dh}{dT} \qquad (6)$$

where h is a function of temperature only, is used to restate Eq. (5) as follows:

$$\frac{dQ}{c_p T} = \frac{dT}{T} + \frac{d\,(V^2/2)}{c_p T} \qquad (7)$$

The basic momentum theorem for the fluid flowing steadily through the control surface is:

$$\sum \underline{F} = \oint \rho(\underline{V} \cdot d\underline{A})\underline{V} \qquad (8)$$

The forces on the fluid within the control volume are due to normal and sidewall pressures and a sidewall friction. These effect

a change of momentum flux expressed as:

$$dp + \tau_W \frac{dA_W}{A} + \rho VdV = 0 \tag{9}$$

The equation of state is:

$$p = \rho \bar{R} T \tag{10}$$

and may be written:

$$\frac{dp}{p} = \frac{d\rho}{\rho} + \frac{dT}{T} \tag{11}$$

The definition of sonic velocity is:

$$\alpha = \sqrt{\left(\frac{\partial p}{\partial \rho}\right)_S} \tag{12}$$

Since $p = \text{const} (\rho)^{\gamma}$ for the assumed gas undergoing an isentropic process, the speed of sound is also represented as:

$$\alpha = \sqrt{\gamma \bar{R} T} \tag{13}$$

Mach number is defined as the ratio of stream velocity to speed of sound:

$$M^2 = \frac{V^2}{\alpha^2} = \frac{V^2}{\gamma \bar{R} T} \tag{14}$$

and is written:

$$\frac{dM^2}{M^2} = \frac{dV^2}{V^2} - \frac{dT}{T} \tag{15}$$

Reference states such as isentropic stagnation condition and at $M = 1$ are useful in control surface analysis. Stagnation refers to conditions of zero velocity, and the isentropic stagnation state of a

fluid denoted by subscript (o) is that obtained by an adiabatic and reversible slowing-down process to negligible motion. Hence, the energy equation, (Eq. 4), written for two control sections so chosen to make the external work equal to zero:

$$Q + c_p T_1 + \frac{V_1^2}{2} = c_p T_2 + \frac{V_2^2}{2} = c_p T + \frac{V^2}{2} \qquad (16)$$

can be used to obtain the stagnation temperature for state one and two, as:

$$T_{o1} = T_1 + \frac{V_1^2}{2 c_p} \qquad (17)$$

and:

$$T_{o2} = T_2 + \frac{V_2^2}{2 c_p} \qquad (18)$$

If a process is isentropic or adiabatic, the stagnation temperature remains constant, but decreases in the presence of cooling since Q is negative. When reference is made to a fluid at a condition of $M = 1$, a subscript (*) is used.

When the relation for specific heat for a perfect gas:

$$c_p = \frac{\gamma}{\gamma - 1} \bar{R} \qquad (19)$$

is used with the definition of Mach number, note that:

$$V^2 = M^2 a^2 = M^2 (\gamma - 1) c_p T \qquad (20)$$

and hence, Equations (7) and (9) may be written respectively as:

$$\frac{d Q}{c_p T} = \frac{dT}{T} + \frac{\gamma - 1}{2} M^2 \frac{dV^2}{V^2} \qquad (21)$$

and:

$$\frac{dp}{p} = - \frac{\gamma M^2}{2} \frac{dV^2}{V^2} - \frac{\tau_w}{p} \frac{dA_w}{A} \tag{22}$$

Simultaneous solution of the Equations of continuity, state, definition of Mach number, energy and momentum which are (3), (11), (15), (21), and (22) respectively, yields:

$$\frac{dM^2}{M^2} = - \frac{2(1 + \frac{\gamma - 1}{2}M^2)}{1 - M^2} \frac{dA}{A} + \frac{1 + \gamma M^2}{1 - M^2} \frac{dQ}{c_p T} +$$

$$\frac{2(1 + \frac{\gamma - 1}{2}M^2)}{1 - M^2} \frac{\tau_w}{A} \frac{dA_w}{A} \tag{23}$$

This equation may be used to evaluate the actual exit Mach number when expressions for cooling and wall friction effects are available as function of M and a space coordinate. It is noted that in a frictionless and adiabatic flow, $\frac{dM^2}{M^2}$ may be evaluated using the $\frac{dA}{A}$ term, and the exit Mach number obtained represents an ideal for the given exit area. The presence of the denominator $(1 - M^2)$ in Equation (23) is instructive. When $M < 1$, M increases for area decrease, heating and friction. For $M > 1$, M increases for cooling and area increase and decreases with friction.

The integration of Equation (23) is usually accomplished numerically in stepwise fashion with attendant difficulties in the region of $M = 1$ because of the denominator $1 - M^2$ tending to zero. This was eliminated by rearranging Equation (23) to:

$$\frac{1 - M^2}{2(1 + \frac{\gamma - 1}{2}M^2)} \frac{dM^2}{M^2} = -\frac{dA}{A} + \frac{1 + \gamma M^2}{2(1 + \frac{\gamma - 1}{2}M^2)} \cdot \frac{dQ}{c_p T} +$$

$$\mathcal{T}_w \frac{dA_w}{A} \tag{24}$$

where the left hand term was integrable:

$$\int_{M_1}^{M} \frac{1 - M^2}{2(1 + \frac{\gamma - 1}{2}M^2)} \frac{dM^2}{M^2} = -\ln\left\{\left[\frac{1 + \frac{\gamma - 1}{2}M^2}{1 + \frac{\gamma - 1}{2}M_1^2}\right]^{\frac{\gamma + 1}{2(\gamma - 1)}} \cdot \left(\frac{M_1}{M}\right)\right\} \tag{25}$$

Upon integration of the right hand term of Equation (24) the final actual M may be obtained.

One additional property was needed to establish the final state. The stagnation temperature was convenient. From Equation (18), it follows:

$$T_o = T + \frac{V^2}{2c_p} = T\left(1 + \frac{\gamma - 1}{2}M^2\right) \tag{26}$$

or:

$$\frac{dT_o}{T_o} = \frac{dT}{T} + \left(\frac{\gamma - 1}{2} \frac{dM^2}{M^2}\right) \bigg/ \left(1 + \frac{\gamma - 1}{2}M^2\right) \tag{27}$$

When Equations of energy, definition of Mach number and definition of stagnation temperature, which are (7), (20), and (26) respectively, are combined:

$$\frac{dT_o}{T_o} = \frac{1}{1 + \frac{\gamma - 1}{2}M^2} \cdot \frac{d\,Q}{c_p T} \qquad (28)$$

Integration of Equation (28) evaluates T_o.

Nozzle efficiency is a ratio of actual exit kinetic energy to ideal exit kinetic energy. It may be based on the same exit area or pressure. Nozzle efficiency based on exit area is:

$$\text{Eff}_{nA} = \frac{V^2}{V_{SA}^2} = \frac{M^2}{M_{SA}^2}\frac{T}{T_{SA}} \qquad (29)$$

and using Equation (26)

$$\text{Eff}_{nA} = \frac{M^2}{M_{SA}^2}\frac{1 + \frac{\gamma - 1}{2}M_{SA}^2}{1 + \frac{\gamma - 1}{2}M^2}\frac{T_{o_2}}{T_{o_1}} \qquad (30)$$

Nozzle efficiency based on same exit pressure is

$$\text{Eff}_{nP} = \frac{M^2}{M_{SP}^2}\frac{1 + \frac{\gamma - 1}{2}M_{SP}^2}{1 + \frac{\gamma - 1}{2}M^2}\frac{T_{o_2}}{T_{o_1}} \qquad (31)$$

which requires obtaining the actual pressure ratio $\frac{p}{p_1}$, for the actual M and evaluating M_{SP} for the same pressure ratio. An expression for $\frac{p}{p_1}$, may be derived from Equations (2), (10), (14), and (26):

$$\frac{p}{p_1} = \frac{A_1 M_1}{AM}\sqrt{\frac{1 + \frac{\gamma - 1}{2}M_1^2}{1 + \frac{\gamma - 1}{2}M^2}}\sqrt{\frac{T_{o_2}}{T_{o_1}}} \qquad (32)$$

and for isentropic processes

$$\frac{p}{p_1} = \left(\frac{T}{T_1}\right)^{\frac{\gamma}{\gamma-1}} \tag{33}$$

and hence M_{SP} may be obtained using Equation (26) with Equation (33) in the following form:

$$\frac{p}{p_1} = \left[\frac{1 + \frac{\gamma-1}{2}M_{SP}^2}{1 + \frac{\gamma-1}{2}M_1^2}\right]^{\frac{\gamma}{\gamma-1}} \tag{34}$$

Potential Flow

The "core" flow outside the film was assumed to be adiabatic and reversible. Because of the conical sections, the flow was assumed to be a radial type from apparent sink and source points located as shown in Figure 3.
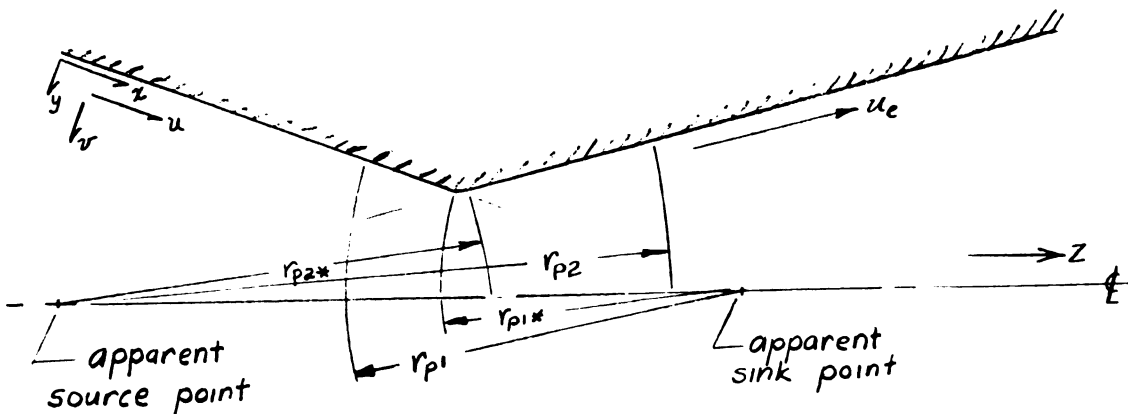
Fig. 3. Sketch of symmetric nozzle with sink and source points for radial flows.

With symmetry about the z-axis spherical coordinates were used. The continuity equation is:

$$\frac{\partial(\rho u_e r_p^2)}{\partial r_p} = 0 \tag{35}$$

Because of dependence of u_e and other properties on r_p only, the flow is irrotational and hence may be called a potential flow.

Integrating Equation (35) gives:

$$\rho u_e = \frac{const}{r_p^2} \tag{36}$$

In accelerating subsonic flow there is a minimum area at which "choked" flow occurs. The polar radius for condition of $M = 1$, is denoted as r_{p*} . Equation (36) may then be written for steady flow as:

$$\frac{r_p^2}{r_{p*}^2} = \frac{\rho_* u_*}{\rho u} = \frac{\rho_* a_*}{\rho u} = \frac{\rho_* a_* a}{\rho u a} \tag{37}$$

with $\dfrac{\rho_*}{\rho} = \left(\dfrac{T_*}{T}\right)^{\frac{1}{\gamma - 1}}$ and $\dfrac{a_*}{a} = \left(\dfrac{T_*}{T}\right)^{1/2}$, Equation (37)

becomes:

$$\frac{r_p^2}{r_{p*}^2} = \frac{1}{M}\left(\frac{T_*}{T}\right)^{\frac{\gamma + 1}{2(\gamma - 1)}} = \frac{1}{M}\left(\frac{T_*}{T_0}\frac{T_0}{T}\right)^{\frac{\gamma + 1}{2(\gamma - 1)}} \tag{38}$$

and using it with Equation (26) since the process is adiabatic:

$$\frac{r_p^2}{r_{p*}^2} = \frac{1}{M}\left[\frac{2}{\gamma + 1}\left(1 + \frac{\gamma - 1}{2}M^2\right)\right]^{\frac{\gamma + 1}{2(\gamma - 1)}} \tag{39}$$

The energy equation is a restatement of constant stagnation enthalpy throughout the adiabatic flow control surface:

$$h_o = h + \frac{v^2}{2} \tag{40}$$

Therefore, the stagnation temperature is constant in the potential flow. The momentum or Euler equation is:

$$\rho u \frac{du}{dr} = - \frac{dp}{dr} \tag{41}$$

The expressions given in this section on potential flow were needed in order to specify the velocity and pressure gradients in the direction of flow at the outer boundary of the laminar layer.

Boundary Layer Flow

Axially symmetric flow for a viscous compressible fluid is described by the following basic equations in cylindrical coordinates (r, z, $\emptyset$) and velocities represented by q.

1. Equation of state:

$$p = \rho \bar{R} T \tag{42}$$

2. Continuity equation:

$$\frac{1}{r} \frac{\partial (q_r \rho r)}{\partial r} + \frac{1}{r} \frac{\partial (\rho r q_z)}{\partial z} \tag{43}$$

3. Energy equation:

$$\rho \left[q_r \frac{\partial h}{\partial r} + q_z \frac{\partial h}{\partial z} \right] = q_r \frac{\partial p}{\partial r} + q_z \frac{\partial p}{\partial z} +$$

$$\frac{1}{r} \frac{\partial}{\partial r} \left(rk \frac{\partial T}{\partial r} \right) + \frac{\partial}{\partial z} \left(k \frac{\partial T}{\partial z} \right) +$$

$$2\mu \left[\left(\frac{\partial q_r}{\partial r} \right)^2 + \left(\frac{q_r}{r} \right)^2 + \left(\frac{\partial q_z}{\partial z} \right)^2 \right] +$$

$$\mu \left[\frac{\partial q_r}{\partial z} + \frac{\partial q_z}{\partial r} \right]^2 - \frac{2}{3} \mu \left[\frac{\partial q_r}{\partial r} + \frac{q_r}{r} + \frac{\partial q_z}{\partial z} \right]^2$$

$$(44)$$

4. Momentum (Navier-Stokes) equations:

$$q_r \frac{\partial q_r}{\partial r} + q_z \frac{\partial q_r}{\partial z} = - \frac{1}{\rho} \frac{\partial p}{\partial r} +$$

$$\frac{1}{\rho} \frac{\partial}{\partial r} \left[\mu \left(2 \frac{\partial q_r}{\partial r} - \frac{2}{3} \frac{1}{r} \frac{\partial(rq_r)}{\partial r} - \frac{2}{3} \frac{\partial q_z}{\partial z} \right) \right] +$$

$$\frac{1}{\rho} \frac{\partial}{\partial z} \left[\mu \left(\frac{\partial q_r}{\partial z} + \frac{\partial q_z}{\partial r} \right) + \frac{2\mu}{\rho r} \left(\frac{\partial q_r}{\partial r} - \frac{q_r}{r} \right) \right]$$

$$(45)$$

$$q_r \frac{\partial q_z}{\partial r} + q_z \frac{\partial q_z}{\partial z} = - \frac{1}{\rho} \frac{\partial p}{\partial z} + \frac{1}{\rho} \frac{\partial}{\partial z}$$

$$\left[\mu \left(2 \frac{\partial q_z}{\partial z} - \frac{2}{3r} \frac{\partial(rq_r)}{\partial r} - \frac{2}{3} \frac{\partial q_z}{\partial z} \right) \right] +$$

$$\frac{1}{\rho r} \frac{\partial}{\partial r} \left[\mu r \left(\frac{\partial q_r}{\partial z} + \frac{\partial q_z}{\partial r} \right) \right] \qquad (46)$$

The difficulty of solution of these differential equations is obvious. Applying laminar boundary layer theory, the equations may be

reduced in complexity when considering a low viscosity fluid in a thin layer along a wall (region of high Reynolds number). It was convenient at this point to change the coordinate system to (x, y) with velocities (u, v) as shown in Figure 3, and rewrite Equations (43), (44), (45), and (46) in dimensionless form.

The following boundary layer assumptions were then applied:

1. $v/u = [0]\ \delta/x$

   where δ is the boundary layer thickness,

2. inertia and viscous forces are of the same order of magnitude:

$$\rho\, u\, \frac{\partial u}{\partial x} = [0]\, \frac{\partial}{\partial y}\left(\mu\, \frac{\partial u}{\partial y}\right)$$

Retaining only high order magnitude terms, the resulting boundary layer equations were:

1. Equation of state:

$$p = \rho \bar{R}T \tag{47}$$

2. Continuity equation:

$$\frac{1}{r}\, \frac{\partial(\rho u r)}{\partial x} + \frac{\partial(\rho v)}{\partial y} = 0 \tag{48}$$

3. Energy equation:

$$\rho\left[u\frac{\partial h}{\partial x} + v\frac{\partial h}{\partial y}\right] = u\frac{\partial p}{\partial x} + \frac{\partial}{\partial y}\left(k\frac{\partial T}{\partial y}\right) + \mu\left(\frac{\partial u}{\partial y}\right)^2 \tag{49}$$

4. Momentum equations:

$$u\frac{\partial u}{\partial x} + v\frac{\partial u}{\partial y} = -\frac{1}{\rho}\frac{\partial p}{\partial x} + \frac{1}{\rho}\frac{\partial}{\partial y}\left(\mu\frac{\partial u}{\partial y}\right) \tag{50}$$

$$\frac{\partial p}{\partial y} = [0] \ 1 \qquad\qquad\qquad (51)$$

The transformation formulae used are given in Appendix A. Because of the length of the expressions, the complete derivation was not included. The above expressions are identical to those for axially symmetric boundary layer flow over bodies of revolution of large radius given in Pai[1]. Pressure is considered to be a function of x only since Equation (51) states that the change of p in the y direction is negligible since $y \leq \mathcal{S}$.

It is possible to reduce the boundary layer Equations (47), (48), (49), and (50) to a form identical for two-dimensional boundary flow for a compressible fluid when the duct radius is large relative to thickness of boundary layer as shown in Figure 4, (so that r may be replaced by R).
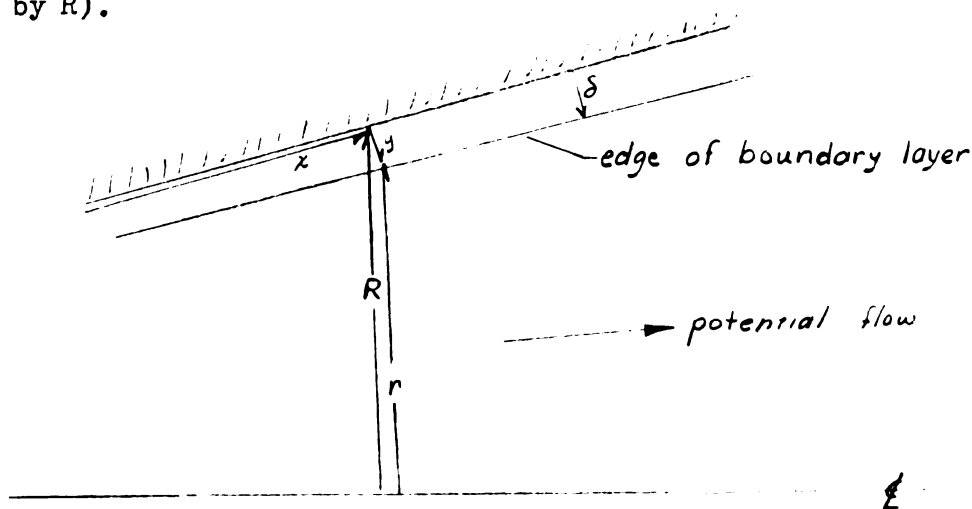
Fig. 4. Sketch of boundary layer in duct.

[1]Pai, Shih-I. Viscous Flow Theory, Vol. I. Laminar Flow. D. Van Nostrand Company, Inc., Princeton, N. J., 1956, p. 141.

This was done using the following Mangler Transformation:[1]

$$x' = L \int_0^{x/L} \frac{R^2}{L^2} \, d(x/L) \tag{53}$$

$$y' = \frac{R}{L} \, y \tag{54}$$

where L is an arbitrary length.

The resulting basic equations are:

1. $p' = \rho' \bar{R} T'$ (55)

2. $\dfrac{\partial(\rho' u')}{\partial x'} + \dfrac{\partial(\rho' v')}{\partial y'} = 0$ (56)

3. $\rho' u' \dfrac{\partial h'}{\partial x'} + \rho' v' \dfrac{\partial h'}{\partial y'} = u' \dfrac{\partial p'}{\partial x'} + \mu \left(\dfrac{\partial u'}{\partial y'} \right)^2 +$

$$\frac{\partial}{\partial y'} \left(k' \frac{\partial T'}{\partial y'} \right) \tag{57}$$

4. $\rho' u' \dfrac{\partial u'}{\partial x'} + \rho' v' \dfrac{\partial u'}{\partial y'} = - \dfrac{\partial p'}{\partial x'} + \dfrac{\partial}{\partial y'} \left(\mu' \dfrac{\partial u'}{\partial y'} \right)$

$$\tag{58}$$

Transformation formulae used are given in Appendix B.

Further coordinate changes may be made with a modified Stewart-son's transformation. This was used by Cohen and Reshotko[2] to obtain

[1]Low, George M. Simplified Methods for Calculation of Compressible Laminar Boundary Layer with Arbitrary Free-Stream Pressure Gradient. NACA TN 2531, 1951, p. 18.

[2]Cohen, Clarence and Eli Reshotko. Similar Solutions for the Compressible Laminar Boundary Layer with Heat Transfer and Pressure Gradient. NACA Report 1293, 1956.

a solution of the steady two-dimensional compressible laminar boundary layer equations. The transformation equations are:

$$x'' = L \int_0^{x'/L} \lambda \, \frac{p_e a_e}{p_0 a_0} \, d(x'/L) \tag{59}$$

$$y'' = \frac{a_e}{a_0} \int_0^{y'} \frac{\wp'}{\wp_0} \, dy' \tag{60}$$

The viscosity law[1] used was:

$$\frac{\mu'}{\mu_0} = \lambda \frac{T'}{T_0} \tag{61}$$

where:

$$\lambda = \sqrt{\frac{T_w}{T_0}} \left(\frac{T_0 + K_{su}}{T_w + K_{su}} \right) \tag{62}$$

Equations (61) and (62) match values from the Sutherland formula for viscosity at the solid boundary. Note that λ is a constant when T_w is constant.

An enthalpy function was defined as

$$S = \frac{h_{st}}{h_0} - 1 \tag{63}$$

with $h_{st} = \frac{(u')^2}{2} + h$ equal to the local stagnation enthalpy.

---

[1]Chapman, Dean and Morris W. Rubesin. Temperature and Velocity Profiles in the Compressible Laminar Boundary Layer with Arbitrary Distribution of Surface Temperature. Jour. Aero. Sci., Vol. 16, No. 9, September 1949, pp. 547-565.

The transformed two-dimensional boundary layer equations (See Appendix C for additional transformation formulae) are:

1. $p'' = \rho'' \bar{R} T''$ (64)

2. $\dfrac{\partial u''}{\partial x''} + \dfrac{\partial v''}{\partial y''} = 0$ (65)

3. $u'' \dfrac{\partial S}{\partial x''} + v'' \dfrac{\partial S}{\partial y''} = \dfrac{\nu_o}{Pr} \Bigg\{ \dfrac{\partial}{\partial y''}\left(\dfrac{\partial S}{\partial y''}\right) - (1 - Pr)\left(\dfrac{\dfrac{\gamma-1}{2}M_e^2}{1 + \dfrac{\gamma-1}{2}M_e^2}\right)\left[\dfrac{\partial}{\partial y''}\left(\dfrac{\partial \left(\dfrac{u''}{u''_e}\right)^2}{\partial y''}\right)\right] \Bigg\}$ (66)

4. $u'' \dfrac{\partial u''}{\partial x''} + v'' \dfrac{\partial u''}{\partial y''} = u''_e \dfrac{\partial u''_e}{\partial x''}(1 + S) + \nu_o \dfrac{\partial}{\partial y''}\left(\dfrac{\partial u''}{\partial y''}\right)$ (67)

A point of interest about the modified Stewartson transformation is that Equation (65) no longer contains density as in Equation (56). Hence, the set of differential equations appear similar, in part, to those for incompressible flow and are identical for an adiabatic core with Pr = 1.

The applicable boundary conditions to Equations (64), (65), (66), and (67) are:

$u''(x'', o) = 0$ $\qquad \lim_{\eta \to \infty} S = 0$

$v''(x'', o) = 0$

$S(x'', o) = S_w$ $\qquad \lim_{\eta \to \infty} u'' = u''_e$ (68)

Cohen and Reshotko[1] next made a final transformation of the boundary

layer equations using:

$$u''_e = c(x'')^m \tag{69}$$

$$S = S(\eta) \tag{70}$$

$$\psi'' = f(\eta) \sqrt{\frac{2 \nu_o u_e'' x''}{m + 1}} \tag{71}$$

$$\eta = y'' \sqrt{\frac{m + 1}{2} \frac{u_e''}{\nu_o x''}} \tag{72}$$

and obtained:

$$\frac{\partial^3 f}{\partial \eta^3} + f \frac{\partial^2 f}{\partial \eta^2} = \beta \left[\left(\frac{\partial f}{\partial \eta} \right)^2 - 1 - S \right] \tag{73}$$

$$\frac{\partial^2 S}{\partial \eta^2} + Pr \, f \frac{\partial S}{\partial \eta} = (1 - Pr) \left[\frac{\frac{\gamma - 1}{2} M_e^2}{1 + \frac{\gamma - 1}{2} M_e^2} \right] \cdot$$

$$\left[\frac{\partial f}{\partial \eta} \frac{\partial^3 f}{\partial \eta^3} + \left(\frac{\partial^2 f}{\partial \eta^2} \right)^2 \right] \tag{74}$$

where $\beta = \dfrac{2m}{m + 1}$.

Hence, a set of ordinary differential equations were obtained,

dependent only on the variable η , if the right hand member of

Equation (74) were taken as zero or a function of η . The case of

Pr = 1 was taken, and results of their solution tabulated for different

values of S_w (dependent on wall and potential stream stagnation temp-

erature) and β (a measure of pressure gradient).

---

[1] Cohen and Reshotko, op. cit.

The boundary conditions for Equations (73) and (74) when $Pr = 1$ are:

$$f(o) = 0 \qquad\qquad \lim_{\eta \to \infty} \frac{\partial f}{\partial \eta} = 1$$

$$\frac{\partial f(o)}{\partial \eta} = 0$$

$$\qquad\qquad\qquad \lim_{\eta \to \infty} S = 0$$

$$S(o) = S_w \tag{75}$$

The values of m in $u_e" = c(x")^m$ that would be needed to describe the subsonic potential velocity in the given nozzle are as follows:

1. At low Mach numbers

$$\text{where } \frac{du_e}{dx} \cong 0 \qquad\qquad \text{then } m \cong 0$$

2. At M increasing to one

$$\text{where } u_e = \text{finite value} \qquad \text{then } m \gg 1$$

An expression for m may be obtained by differentiating Equation (69) with respect to $x"$:

$$\frac{du_e"}{dx"} = mc(x")^{m-1} = \frac{mu_e"}{x"} \tag{76}$$

and

$$m = \frac{du_e"}{dx"} \cdot \frac{1}{u_e"} \cdot x"$$

or

$$m = \frac{du_e}{dx} \cdot \frac{R^2}{L^2} \cdot \frac{1}{u_e} \cdot \frac{a_o^3}{a_e^3} \frac{P_o}{P_e} \int_o^x \frac{a_e P_e}{a_o P_o} \frac{R^2}{L^2} dx \tag{77}$$

where

$$\frac{du_e''}{dx''} = \frac{a_o^4}{a_e^4} \frac{1}{\lambda} \frac{p_o}{p_e} \frac{du_e}{dx'}$$

$$\frac{dx'}{dx} = \frac{R^2}{L^2}$$

$$x'' = \lambda \int_0^x \frac{a_e p_e}{a_o p_o} \cdot \frac{R^2}{L^2} \cdot dx$$

$$u_e'' = \frac{a_o}{a_e} u_e$$

Equation (77) may be used to obtain values for m. In the first example, if u_e and x are not zero, and $\frac{du_e}{dx} \cong 0$, then $m \cong 0$. This is analogous to flat plate flow where u_e = constant and $\frac{dp_e}{dx} = 0$. In the second example, $\frac{du_e}{dx} \longrightarrow \infty$ as $M_e \longrightarrow 1$, hence m becomes very large. Since m must be a constant, the transformation Equations (69), (70), (71), and (72) were not useful as such for the given problem.

It was found that if the following potential velocity distribution was assumed

$$u_e'' = c_1 e^{K_1 \frac{x''}{L}} \tag{78}$$

and was used with following transformations

$$\psi'' = f(\eta) \sqrt{\frac{2u_e'' \nu_o L}{K_1}} \tag{79}$$

$$S = S(\eta)$$

$$y'' = \eta \sqrt{\frac{2\nu_o L}{K_1 u_e''}}$$

in Equations (64), (65), (66), and (67), the transformed equations became

$$\frac{\partial^3 f}{\partial \eta^3} + f \frac{\partial^2 f}{\partial \eta^2} = 2 \left[\left(\frac{\partial f}{\partial \eta} \right)^2 - (1 + S) \right] \tag{80}$$

$$\frac{\partial^2 S}{\partial \eta^2} + Prf \frac{\partial S}{\partial \eta} = (1 - Pr) \left[\left(\frac{(\gamma - 1)M_e^2}{1 + \frac{\gamma - 1}{2}M_e^2} \right) \right.$$

$$\left. \left(\frac{\partial f}{\partial \eta} \frac{\partial^3 f}{\partial \eta^3} + \left(\frac{\partial^2 f}{\partial \eta^2} \right)^2 \right) \right] \tag{81}$$

with the following boundary conditions

$$f(o) = 0 \qquad \qquad \frac{\partial f(o)}{\partial \eta} = 0$$

$$S(o) = S_w$$

$$\lim_{\eta \to \infty} S = 0 \qquad \qquad \lim_{\eta \to \infty} \frac{\partial f}{\partial \eta} = 1 \tag{82}$$

The transformations and detailed substitutions to obtain Equations (80), (81) are given in Appendix D.

Since the transformed Equations (80), (81) are the same set of simultaneous non-linear ordinary differential equations of fifth order with the same boundary conditions as in Equations (73), (74) with $\beta = 2$ and $Pr = 1$, the solutions for f and S are the same.

The one remaining point to be satisfied was that the velocity distribution as defined in Equation (78) described the given potential flow to be investigated. The derivation required that K_1 be a constant. Further discussion of this point may be found in the Procedure Section.

Temperature and velocity gradients were desired at the wall. They may be expressed as follows:

Since $\dfrac{\partial f}{\partial \eta} = \dfrac{u''}{u_e''}$, the velocity gradient is:

$$\frac{\partial u}{\partial y} = \frac{\alpha_e^2}{\alpha_o^2} \frac{\partial^2 \psi''}{\partial y''^2} \frac{\rho}{\rho_o} \frac{R}{L} \tag{83}$$

and further, at the wall,

$$\left(\frac{\partial u}{\partial y}\right)_w = \left(\frac{\alpha_e}{\alpha_o}\right)^2 \frac{\rho_w}{\rho_o} u_e'' \left(\frac{\partial^2 f}{\partial \eta^2}\right)_w \sqrt{\frac{K_1 u_e''}{2\nu_o L}} \frac{R}{L} \tag{84}$$

An expression for temperature is needed. Using the following:

$$\frac{T_{st}}{T_e} = \frac{\alpha^2 + \dfrac{\gamma-1}{2} u'^2}{\alpha_e^2} = \frac{T_{st}}{T_o}\frac{T_o}{T_e} = (1+S)(1 + \frac{\gamma-1}{2}M_e^2)$$

$$\frac{T_{st}}{T_e} = \frac{T + \dfrac{u'^2}{2c_p}}{T_e}$$

hence $\dfrac{T}{T_e} = (1+S)(1 + \dfrac{\gamma-1}{2}M_e^2) - \dfrac{\gamma-1}{2}\dfrac{u_e^2}{\alpha_e^2}\dfrac{u^2}{u_e^2}$

or $\quad \dfrac{T}{T_o} = (1+S) - \left(\dfrac{\dfrac{\gamma-1}{2}M_e^2}{1 + \dfrac{\gamma-1}{2}M_e^2}\right)\left(\dfrac{\partial f}{\partial \eta}\right)^2 \tag{85}$

Therefore, the temperature gradient is

$$\left(\frac{\partial T}{\partial y}\right)_x = T_o \left(\frac{\partial s}{\partial y}\right)_x$$

$$\left(\frac{\partial T}{\partial y}\right)_w = T_o \left(\frac{\partial s}{\partial \eta}\right)_w \frac{\alpha_e}{\alpha_o}\frac{\rho_w}{\rho_o}\frac{R}{L}\sqrt{\frac{K_1 u_e''}{2\nu_o L}} \tag{86}$$

since $\dfrac{\partial f}{\partial \eta} = 0$ at the wall.

One method used to check some of the data obtained was to evaluate the dimensionless parameter $c_{f_w} \sqrt{Re_w}$ and compare with available data for flat plate flow. The following expression was derived in the x,y coordinate system for wall conditions.

The skin friction coefficient is defined as

$$c_f = \frac{\tau_w}{(1/2)\,\rho_w\,u_e^2} \tag{87}$$

and shear stress in the laminar flow is defined as

$$\tau = \mu\,\frac{\partial u}{\partial y} \tag{88}$$

Substituting Equations (83), (88) into (87) for wall conditions:

$$c_f = \frac{\left[\lambda\mu_0\,\dfrac{T}{T_0}\left(\dfrac{\alpha_e}{\alpha_0}\right)^2 u_e{}'' \dfrac{\partial^2 f}{\partial\eta^2}\sqrt{\dfrac{K_1 u_e''}{2\,\nu_0 L}}\,\dfrac{p}{p_0}\,\dfrac{R}{L}\right]_w}{1/2\,\rho_w\,(u_e'')^2} \tag{89}$$

The definition of Reynolds number is

$$Re_w = \frac{u_e x}{\nu_w} \tag{90}$$

and combining Equations (89), (90)

$$c_{f_w}\sqrt{Re_w} = \frac{\lambda\mu_0\,\dfrac{p_w}{p_0}\left(\dfrac{\alpha_e}{\alpha_0}\right)^2 u_e{}''\left(\dfrac{\partial^2 f}{\partial\eta^2}\right)\dfrac{R}{L}\sqrt{\dfrac{K_1 u_e'' \cdot u_e\,x}{2\,\nu_0\,L\,\nu_w}}}{1/2\,\rho_w\,(u_e'')^2} \tag{91}$$

Since K_1 in the velocity distribution is

$$K_1 = \frac{\ln \ u_e{''}/c_1}{x{''}/L} = \frac{\ln \ u_e{''}/c_1}{\int_0^{x/L} \lambda \frac{a_e p_e}{a_o p_o} \cdot \frac{R^2}{L^2} \ d(x/L)} \qquad , \qquad (92)$$

Equation 91 may be written

$$c_{f_w} \sqrt{Re_w} = \sqrt{2} \left(\frac{\partial^2 f}{\partial \eta^2} \right)_w$$

$$\cdot \frac{R}{L} \sqrt{\frac{x/L \cdot \ln \frac{u_e{''}}{c_1} \cdot \left(\frac{T_e}{T_o} \right)^{\frac{3\gamma-1}{2(\gamma-1)}}}{\int_0^{x/L} \left(\frac{T_e}{T_o} \right)^{\frac{3\gamma-1}{2(\gamma-1)}} \frac{R^2}{L^2} \ d(x/L)}} \cdot (93)$$

Finally, expressions for $\frac{dQ}{c_p T}$ and $\frac{\tau_w \ dA_w}{A}$ were needed for

use in Equation (24). These terms depend upon velocity and temperature gradients in the fluid adjacent to the wall. The gradients were obtainable upon solution of the laminar boundary layer equations.

Fourier's Law of heat conduction was used

$$q_w = - k \left(\frac{\partial T}{\partial y} \right)_w \qquad (94)$$

to obtain

$$\frac{dQ}{c_p T_e} = \frac{- k \left(\frac{\partial T}{\partial y} \right)_w}{w \ c_p T_e} \ dA_w \qquad (95)$$

The following substitutions may be used:

$$\frac{dA_w}{A} = \frac{\sin^2 \vartheta \ R \ dx}{\rho_e u_e (1 - \cos \vartheta) R^2} \tag{96}$$

$$\frac{k}{c_p} = \mu \tag{97}$$

$$p = p_e \tag{98}$$

along with Equations (10), (14), (61), (86), (92) and isentropic $p - T$ relations to obtain the heat transfer term:

$$\frac{dQ}{c_p T} = - \frac{\sin^2 \vartheta}{1 - \cos \vartheta} \cdot$$

$$\sqrt{\frac{\dfrac{\vartheta_0 \lambda}{2 L a_0} \ln \dfrac{u_e''}{c_1}}{M_e \displaystyle\int_0^{x/L} \left(\dfrac{1}{1 + \dfrac{\gamma - 1}{2} M^2}\right)^{\frac{3\gamma - 1}{2(\gamma - 1)}} \dfrac{R^2}{L^2} \ d(x/L)}}$$

$$\cdot \left(\frac{\partial s}{\partial \eta}\right)_w \ d(x/L) \tag{99}$$

The skin friction term may be obtained using Equations (14), (61), (84), (88) and (96):

$$\frac{\mathcal{T}_w\, dA_w}{A} = \gamma M^2 \cdot \frac{\sin^2 \vartheta}{1 - \cos \vartheta}\left(\frac{T_e}{T_o}\right) \cdot$$

$$\sqrt{\frac{\dfrac{\nu_o \lambda}{2La_o}\ln\dfrac{u_e''}{c_1}}{M_e\displaystyle\int_0^{x/L}\left(\dfrac{1}{1 + \dfrac{\gamma - 1}{2}M^2}\right)^{\frac{3\gamma - 1}{2(\gamma - 1)}}\dfrac{R^2}{L^2}\,d(x/L)}}$$

$$\cdot\left(\frac{\partial^2 f}{\partial \eta^2}\right)_w d(x/L) \qquad (100)$$

Hence Equation (24) may be written:

$$\frac{1 - M^2}{2\left(1 + \dfrac{\gamma - 1}{2}M^2\right)}\frac{dM^2}{M^2} = -\frac{dA}{A} + \frac{\sin^2 \vartheta}{1 - \cos \vartheta} \cdot$$

$$\sqrt{\frac{\dfrac{\nu_o \lambda}{2La_o}\ln\dfrac{u_e''}{c_1}}{M_e\displaystyle\int_0^{x/L}\left(\dfrac{1}{1 + \dfrac{\gamma - 1}{2}M^2}\right)^{\frac{3\gamma - 1}{2(\gamma - 1)}}\dfrac{R^2}{L^2}\,d(x/L)}}$$

$$\left[-\frac{1 + \gamma M^2}{2\left(1 + \dfrac{\gamma - 1}{2}M^2\right)}\left(\frac{\partial s}{\partial \eta}\right)_w + \frac{\gamma M^2}{1 + \dfrac{\gamma - 1}{2}M^2}\left(\frac{\partial^2 f}{\partial \eta^2}\right)_w\right]d(x/L)$$

$$(101)$$

When a constant wall temperature, inlet stagnation conditions, and nozzle angles are given, the following parameters are fixed: ν_o, λ, a_o, L, γ, $\left(\dfrac{\partial s}{\partial \eta}\right)_w$, $\left(\dfrac{\partial^2 f}{\partial \eta^2}\right)_w$, and ϑ. Equation (101) is then usable to find M for a given change in x.

Knowing variation of M with x, Equations (28) and (99) may be combined:

$$\frac{dT_o}{T_o} = -\frac{\sin^2 \vartheta}{1 - \cos \vartheta}\left(\frac{1}{1 + \dfrac{\gamma - 1}{2}M^2}\right) \cdot$$

$$\sqrt{\frac{\dfrac{\nu_o \lambda}{2La_o} \ln \dfrac{u_e''}{c_1}}{M_e \displaystyle\int_0^{x/L} \left(\frac{1}{1 + \dfrac{\gamma - 1}{2}M^2}\right)^{\frac{3\gamma - 1}{2(\gamma - 1)}} \dfrac{R^2}{L^2}\, d(x/L)}} \left(\frac{\partial s}{\partial \eta}\right)_w d(x/L)$$

$$\tag{102}$$

to allow solution for T_o.

PROCEDURE IN CALCULATIONS

For convenience, data was evaluated by specifying the ideal Mach number and then obtaining values for displacement, area, etc.. This was done because of the difficulty in solving for M_{SA} explicitly in most of the gas dynamic equations.

The origin for x, displacement along the wall, was chosen at $M = 0.001$, where fluid properties had essentially stagnation values. Using this initial condition, the constant c in Equation (78) must be equal to $u_e''_{\frac{x}{L} = 0}$. The ratio of $\frac{u_e''}{c_1}$ in Equation (92) may be written:

$$\frac{u_e''}{c_1} = \frac{u_e''}{u_e''_{\frac{x}{L} = 0}} = \frac{u_e'}{\alpha_e} \frac{\alpha_0}{u_e''} = \frac{M_e}{M_e {}_{\frac{x}{L} = 0}} \tag{103}$$

With reference to Figure 1, useful relations between space coordinates were:

$$R_1 = (r_{p1}* + L_1 - x) \sin \theta_1$$

$$R_2 = (r_{p2}* + x - L_1) \sin \theta_2 \tag{104}$$

where subscripts 1 and 2 refer to converging and diverging sections respectively.

For $A_{1*} = A_{2*}$, then

$$\frac{r_{p2}*}{r_{p1}*} = \sqrt{\frac{1 - \cos \theta_1}{1 - \cos \theta_2}} \tag{105}$$

and displacement in terms of area ratios become:

$$\frac{x}{r_{pl*}} = \sqrt{\left(\frac{A}{A^*}\right)_{\frac{x}{r_{pl*}} = 0}} - \sqrt{\frac{A}{A^*}} \qquad \text{for } M < 1 \qquad (106)$$

$$\frac{x}{r_{pl*}} = \sqrt{\frac{1 - \cos \theta_1}{1 - \cos \theta_2}} \left(\sqrt{\frac{A}{A^*}} - 1 \right) + \frac{L_1}{r_{pl*}} \quad \text{for } M > 1 \qquad (107)$$

For calculation purposes, such as in Equation (101), the arbitrary

length L was considered as r_{pl*} .

Area ratios were obtained using Equation (39). Since the term

$$\left(\frac{1}{1 + \frac{\gamma - 1}{2} M^2} \right)$$ appeared regularly, it was convenient, from Equation

(26), to tabulate its equivalent as $\frac{T_{SA}}{T_o}$.

Logarithmic and anti-logarithmic data were obtained by use of

tables[1] and the logarithmic series for ln (1 + x).

For purposes of evaluating effects of losses, the nozzle entrance

was taken where $M_{SA} = 0.1$. However, the integral under the radical

sign in Equations (101) and (102) had to be evaluated from the origin

x = 0. In Appendix E, Table I, small intervals were taken and data

evaluated to obtain this integral and the variation of K_1. The inte-

gration was approximated by summing the product of the average value

of the integrand, and the displacement, for a small interval. The

change in the integral was negligible after $M_\theta > 0.5$. These values ob-

tained by the previously described method of integration were found to

be quite satisfactory when checked in the interval of 0.001 < M < 0.1

---

[1]Table of Natural Logarithms, Vol. I, National Bureau of Standards, 1941.

(where the large change occurs and $\left(\dfrac{T_e}{T_o}\right)^{4.0}$ has little change) using

$\gamma = 1.4$ with:

$$\int_0^{x/r_{pl*}} \left(\frac{T_e}{T_o}\right)^{4.0} \frac{R^2}{r_{pl*}^2} \, d\left(\frac{x}{r_{pl*}}\right) = \overline{\left(\frac{T_e}{T_o}\right)^{4.0}} \sin^2 \theta_1 \int_0^{x/r_{pl*}} \left(\frac{A}{A^*}\right)^2 d\left(\frac{x}{r_{pl*}}\right) \quad (108)$$

and integrating the right hand expression:

$$= \overline{\left(\frac{T_e}{T_o}\right)^{4.0}} \sin^2 \theta_1 \left[\left(\frac{A}{A^*}\right)^2 \frac{x}{r_{pl*}} - \left(\frac{A}{A^*}\right)\left(\frac{x}{r_{pl*}}\right)^2 + 1/3 \left(\frac{x}{r_{pl*}}\right)^3\right]$$

$$(109)$$

The K_1 variation may be seen in column (7) of Table I, Appendix E. Although not of constant value, it was considered that the variation was not excessive in the range of Mach number to be considered, especially with primary interest in $M > 1$. K_1 was considered as a constant and average values were used for given small intervals. Therefore, the integration results[1] of Equations (73) and (74) for $\beta = 2$ and Pr = 1 were taken as applicable to Equations (80) and (81) for Pr = 1 The data used were:

$$\left(\frac{\partial^2 f}{\partial \eta^2}\right)_w = 1.6870 \quad \text{and} \quad \left(\frac{\partial S}{\partial \eta}\right)_w = 0 \qquad \text{when } \frac{T_w}{T_o} = 1.0$$

$$= 1.3329 \qquad\qquad\qquad = 0.2304 \qquad\qquad = 0.6$$

$$= 0.9480 \qquad\qquad\qquad = 0.4331 \qquad\qquad = 0.2$$

$$(110)$$

---

[1] Cohen and Reshotko, _op. cit._

As shown in Equation (30) it was convenient to express efficiency in terms of actual exit Mach number M. To obtain this, Equation (101) had to be integrated. Note that if substitutions are made in Equation (101), using Equations (103) and (110), the only variables are M and x. Numerical methods could be used to integrate this equation. However, calculations were based on the assumption that very small error would be introduced by using ideal Mach numbers in the coefficient of d(x/L) in place of actual M, since effects of friction and heat transfer were expected to be quite small compared with the change in M due to area change.

From Equation (101), for an adiabatic and frictionless process, the integrated expression for actual area change is identical to that given in Equation (25) in terms of ideal Mach number (M_{SA}), based on area change only. Hence, a solution of Equation (101) was taken to be:

$$-\ln \left[\frac{1 + \frac{\gamma - 1}{2}M^2}{1 + \frac{\gamma - 1}{2}M_{SA}^2} \right]^{\frac{\gamma + 1}{2(\gamma - 1)}} \frac{M_{SA}}{M} = \frac{\sin^2 \theta}{(1 - \cos \theta)} \sqrt{\frac{\mathcal{D}_0 \lambda}{2La_0}} \cdot$$

$$\sum (\bar{B}) \, \Delta (x/L) \qquad (111)$$

where $(\bar{B})$ = average value of B for the (x/L) interval

$$= \sqrt{\frac{\ln \frac{M_{SA}}{0.001}}{M_{SA} \int_0^{x/L} \left(\frac{T_e}{T_0}\right)^{\frac{3\gamma - 1}{2(\gamma - 1)}} \frac{R^2}{L^2} \, d(x/L)}} \cdot$$

$$\left(- \frac{1 + \gamma M_{SA}^2}{2\left(1 + \frac{\gamma - 1}{2}M_{SA}^2\right)} \left(\frac{\partial s}{\partial \eta}\right)_w + \frac{\gamma M_{SA}^2}{1 + \frac{\gamma - 1}{2}M_{SA}^2} \left(\frac{\partial^2 f}{\partial \eta^2}\right)_w \right)$$

and $L = r_{pl}*$

Intervals of 0.05 for M_{SA} were taken between $0.1 \le M \le 3.0$.

Calculated data using Equation (106) for one set of initial conditions, $\theta_2 = 15°$, $10°$, and $5°$ and $T_w/T_o = 1.0$, 0.6, 0.2 are given in

Appendix E, Table IV. Stagnation temperature Equation (102) was evaluated in a similar manner, with calculated data given in

Appendix E, Table IV. Results of $\frac{T_{o_2}}{T_{o_1}}$, M actual and Eff_{na} are

given in Table V, with the nozzle efficiency values obtained by using Equation (30).

Some values of nozzle efficiency based on same exhaust region pressure were obtained by:

1. obtaining p/p_1 using M actual in Equation (32).

2. calculating M_{sp} for same pressure ratios using Equation (34).

3. evaluating Eff_{np} for values of M_{sp}, M Actual, and T_{o_2}/T_{o_1} using Equation (31).

Values of the parameter $c_{fw}\sqrt{Re_w}$ were evaluated using previously obtained data in Equation (93) given in Appendix E, Table I.

PRESENTATION AND DISCUSSION OF RESULTS

Using calculation procedures previously described, results were
obtained for:

1. $c_{f_w} \sqrt{Re_w}$

2. Nozzle efficiency based on same exit area for several

   values and constant wall temperature, exit angle and

   parameter Δ.

3. Nozzle efficiency based on same exit pressure.

These values were dependent on the effects of skin friction and
heat transfer at the smooth walls of large radius occurring in a com-
pressible fluid of $\gamma = 1.4$ and $Pr = 1.0$ expanding in a continuous
manner to the exhaust region pressure.

The comparison of $c_{f_w} \sqrt{Re_w}$ for the given flow to that of flat
plate flow where external velocity is constant and pressure gradient
zero, shown in Figure 5, was considered as adequate. It is reasonable
that the initial flow in the entrance of the converging section ap-
proaches flat plate flow behavior since the axial pressure gradient is
essentially zero at those cross sections. The effect of cold walls in
decreasing the $c_{f_w} \sqrt{R_{ew}}$ was consistent since c_{f_w} becomes very small
in larger M as the wall Reynolds number must increase rapidly due to
increases in x and u_e.

In Figure 6, a graphical presentation of values of the three terms
in Equation (111) at various downstream locations
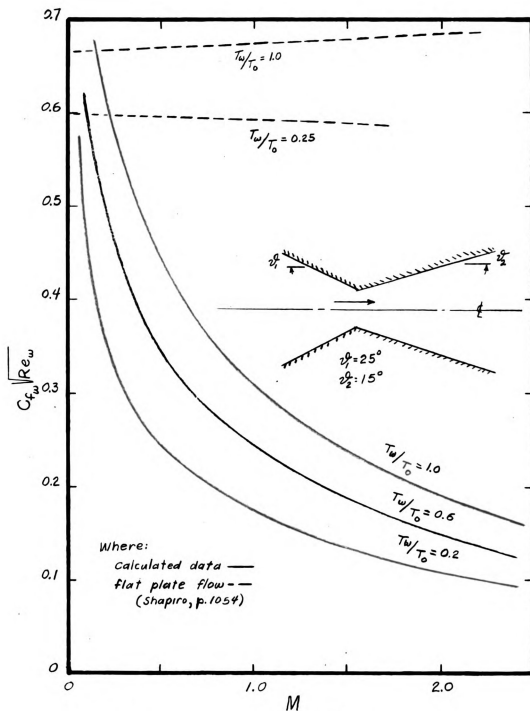
Fig. 5. Comparison of $c_{f_w} \sqrt{Re_w}$ values for flat plate and given nozzle laminar boundary flow.
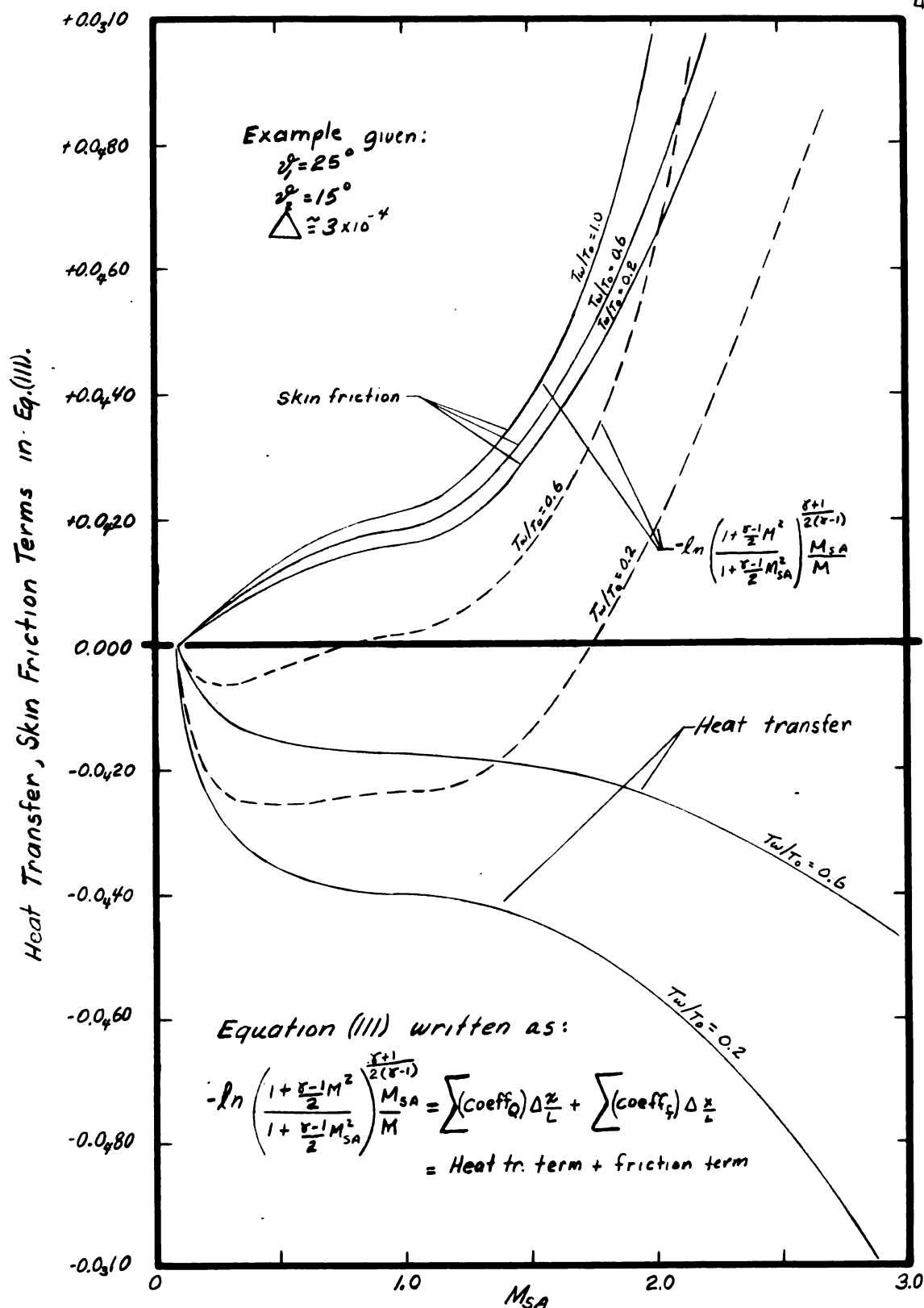
Fig. 6. Graphical presentation of values of each term in Equation (111), and variation with M_{SA}.

was of interest. In both cases of cold walls, the heat transfer term had the dominant role of influence on actual Mach number in the subsonic flow, and with lower temperature conditions, extended its influence into the supersonic region. At a point of zero net effects, it should be noted that the state is not the same as the ideal because of the frictional effects on pressure even though Mach numbers are the same.

A parameter $\triangle$ was defined because of the many possible combinations of other parameters in Equation (111). The defined parameter used consists of

$$\triangle = \sqrt{\frac{\nu_0 \lambda \sin \theta_2 (1 - \cos \theta_1)}{2 R_{min} \alpha_0 (1 - \cos \theta_2)}} \qquad (112)$$

Resultant $\triangle$ values for various possible operating and given conditions are presented in Table 1. The choice of 10 psia low pressure would be consistent with a condition of operation of jet exhaust nozzles at high altitudes where the exhaust region pressure is quite low relative to sea level atmospheric conditions. The following summarizes the changes in $\triangle$ parameter resulting from changes in individual parameters:

Parameter increased	$\triangle$
throat radius (R_{min})	decreased

Table 1

Values of Parameter Δ for Different Given Conditions

R_{min} = 3 in.

T_o	$\theta_2 = 15°$		$\theta_2 = 5°$	
	$p_o = 10$	$p_o = 600$	$p_o = 10$	$p_o = 600$
1200	0.0_389931	0.0_311610	0.0_215616	0.0_319571
2500	0.0_213474	0.0_317395	0.0_223398	0.0_330207
3600	0.0_213474	0.0_321135	0.0_228427	0.0_336699
4200	0.0_217750	0.0_322915	0.0_230822	0.0_339791

R_{min} = 6 in.

T_o	$\theta_2 = 15°$		$\theta_2 = 5°$	
	$p_o = 10$	$p_o = 600$	$p_o = 10$	$p_o = 600$
1200	0.0_363591	0.0_482095	0.0_211042	0.0_313838
2500	0.0_39527	0.0_312300	0.0_216545	0.0_321360
3600	0.0_211577	0.0_314945	0.0_220101	0.0_325950
4200	0.0_212551	0.0_316203	0.0_221794	0.0_328136

R_{min} = 15 in.

T_o	$\theta_2 = 15°$		$\theta_2 = 5°$	
	$p_o = 10$	$p_o = 600$	$p_o = 10$	$p_o = 600$
1200	0.0_340218	0.0_451921	0.0_369837	0.0_487524
2500	0.0_360258	0.0_477793	0.0_210464	0.0_313509
3600	0.0_373213	0.0_494519	0.0_212713	0.0_316412
4200	0.0_379380	0.0_310248	0.0_213784	0.0_317795

where $\Delta = \sqrt{\dfrac{\nu_o \lambda \sin \theta_2 (1 - \cos \theta_1)}{2 R_{min} \alpha_o (1 - \cos \theta_2)}}$

$\theta_2 = 25°$ $\qquad \gamma = 1.4$ $\qquad \bar{R} = 53.4$ $\qquad T_o$ in °R

$\dfrac{T_w}{T_o} = 1.0$ $\qquad k_{su} = 198.6$ $\qquad p_o$ in psia

Exhaust section angle (Θ_2) decreased

Stagnation pressure (p_0) decreased

Stagnation temperature (T_0) increased

Viscosity constant (λ) increased
   (Variation not shown in Table 1)

Effects of skin friction and heat transfer on exit velocity were expressed in terms of effects on nozzle efficiency. Values of efficiency, based on design area, for ideal exit Mach numbers of 1.5, 2.0, 2.5, and 3.0 are given in Figures 7, 8, 9, and 10 respectively. Other calculations substantiate that the linear curves may be extended in increasing $\triangle$ direction to at least 0.0_23. The resulting curves show the effects of friction and heat transfer at walls of different temperatures. In all cases, efficiencies decreased with increases in $\triangle$ parameter. At smaller exit angles of Θ_2 the effects are more distinct as a result of the increased wall area due to greater length. For a given $\triangle$ parameter value, the effects of various T_w/T_0 conditions for Mach numbers greater than twenty were negligible, which leads one to the conclusion that heat transfer effects were negligible or that skin friction was extremely dominant. Under such conditions the effect of heat transfer as an energy loss was negligible. It would not follow that adiabatic and non-adiabatic walls for $\Theta_2 \gtrless 15°$ have the same flow behavior, for cold walls can definitely influence the velocity gradients and hence skin friction in the boundary layer.

Figure 11 expresses the relation between the nozzle efficiencies established on different bases. The value based on same pressure at

1.0000

0.9995

Nozzle Efficiency (Area)

0.9990

$\vartheta_2 = 15°$

$\vartheta_2 = 10°$

$\vartheta_2 = 5°$

$M_{SA} = 1.5$

ϑ_2

$T_w/T_0 = 1.0$ ———

$= 0.6$ – – – –

$= 0.2$ —·—·—

0.9985

$$\triangle = \sqrt{\frac{\vartheta_0 \lambda \; Sin \; \vartheta_2 \; (1 - Cos \; \vartheta_1)}{2 \; R_{min} \; a_0 \; (1 - Cos \; \vartheta_2^0)}}$$

0.9980

0.0_∞ $0.0_3 5$ $0.0_2 1$

$\triangle$
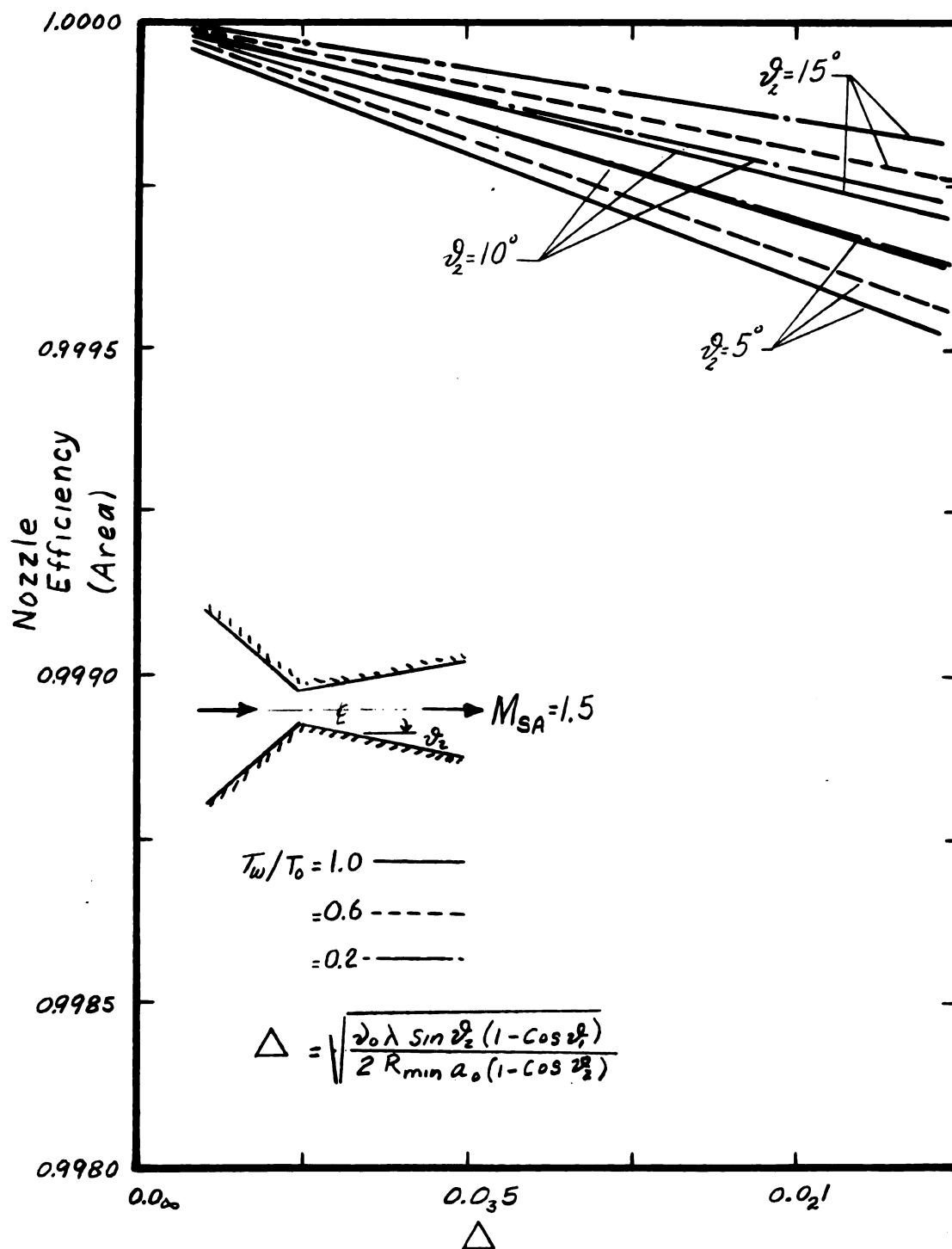
Fig. 7. Variation of nozzle efficiency with parameter
for exit $M_{SA} = 1.5$.
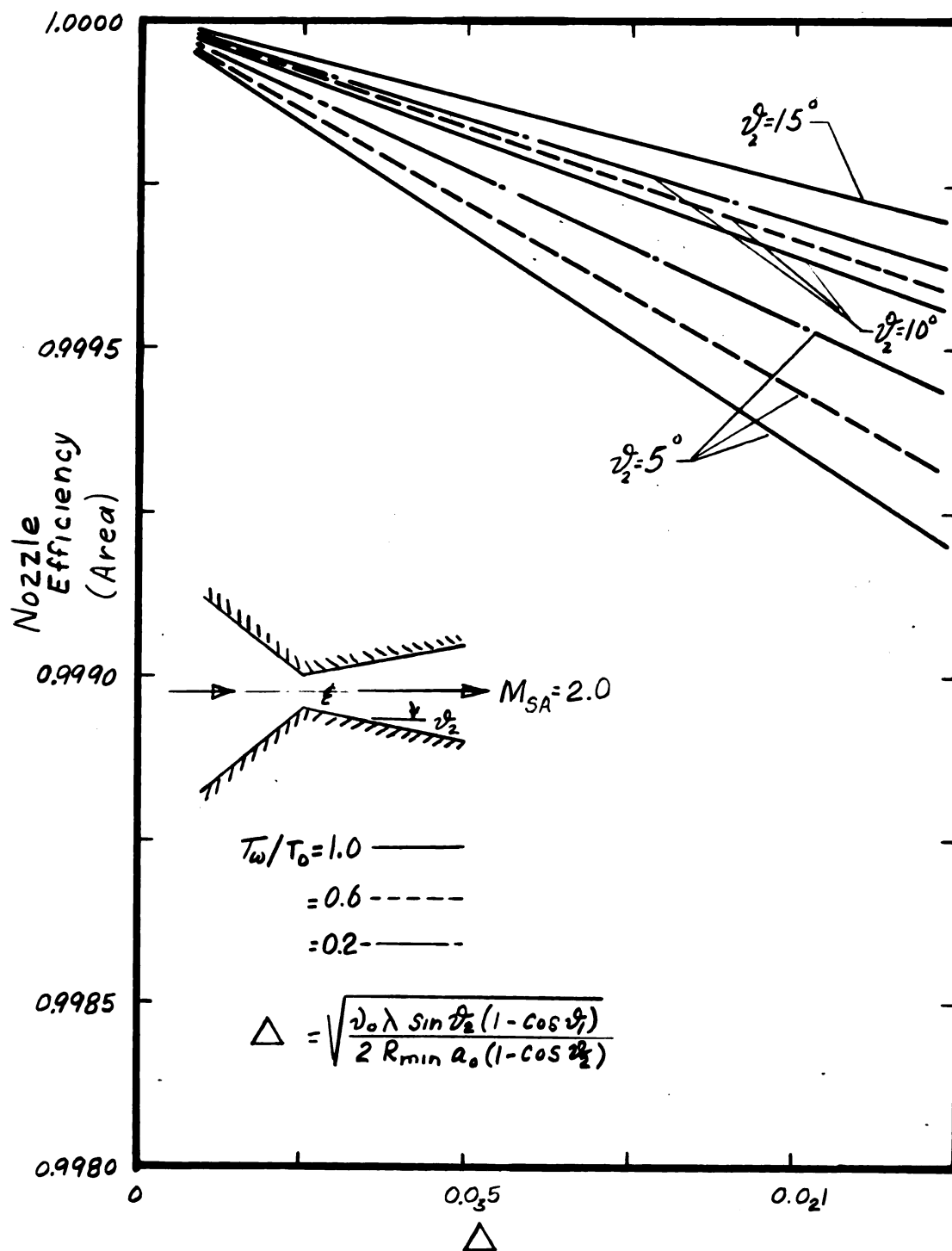
Fig. 8. Variation of nozzle efficiency with parameter for exit M_{SA} = 2.0.

1.0000

0.9995

Nozzle Efficiency (Area)

0.9990

$M_{SA}=2.5$

$\vartheta_2=15°$

$\vartheta_2=10°$

$\vartheta_2=5°$

t

ϑ_2

$T_w/T_0=1.0$ ———

$=0.6$ -----

$=0.2$ ——

0.9985

$$\triangle = \sqrt{\frac{\vartheta_0 \lambda \sin\vartheta_2 (1-\cos\vartheta_1)}{2\,R_{min}\,a_0\,(1-\cos\frac{\vartheta_2}{2})}}$$

0.9980

0   0.0₃5   0.0₂1

$\triangle$

Fig. 9. Variation of nozzle efficiency with parameter
for exit $M_{SA} = 2.5$.

1.0000

0.9995

Nozzle Efficiency (Area)

0.9990

0.9985

$\vartheta_2 = 15°$

$\vartheta_2 = 10°$

$\vartheta_2 = 5°$

$M_{SA} = 3.0$

t

ϑ_2

$T_W/T_0 = 1.0$ ——
$= 0.6$ -----
$= 0.2$ —·—·—

$$\triangle = \sqrt{\frac{\vartheta_0 \lambda \sin \vartheta_2 (1 - \cos \vartheta_1)}{2 R_{min} a_0 (1 - \cos \frac{\vartheta_2}{2})}}$$

0   0.005   0.01

$\triangle$
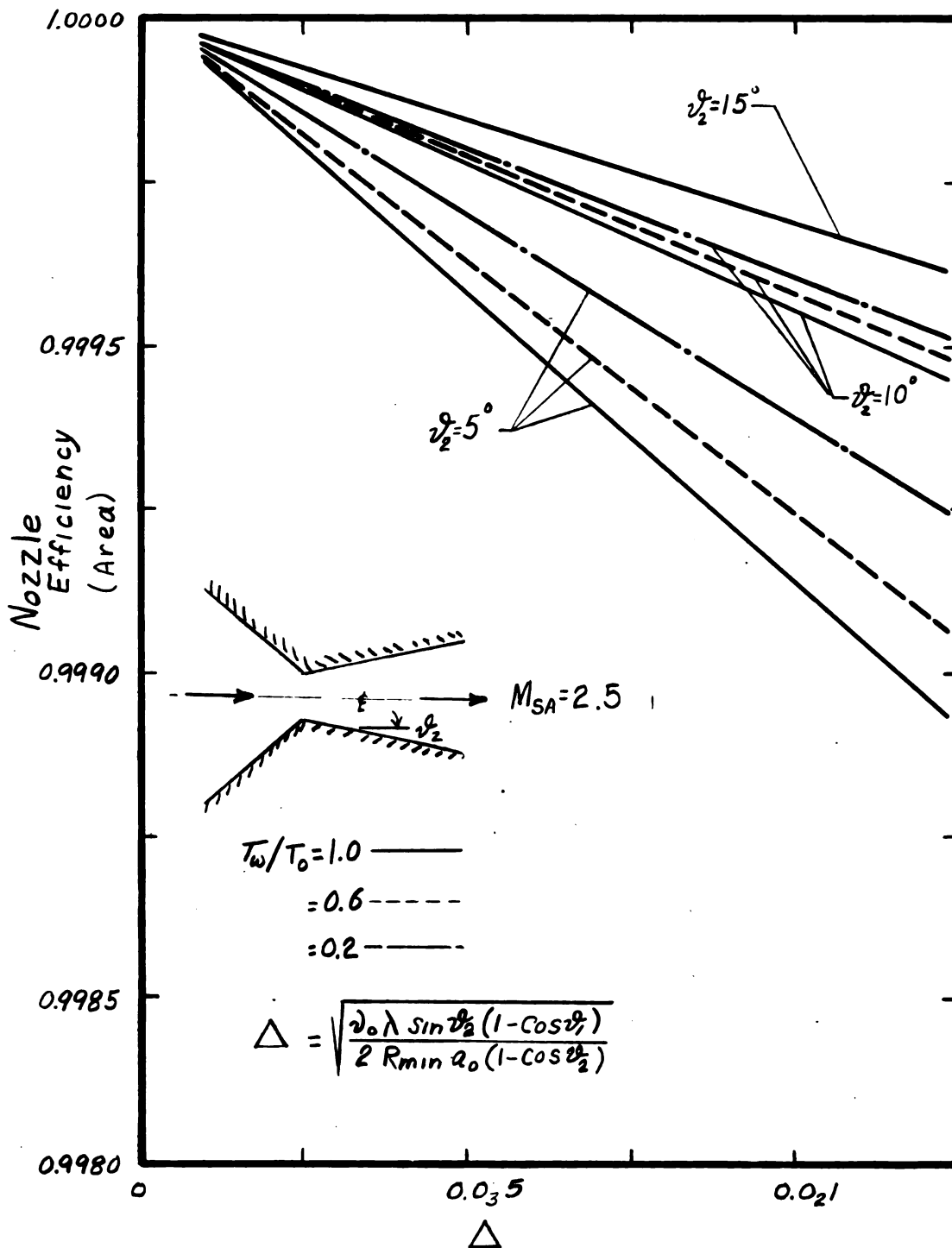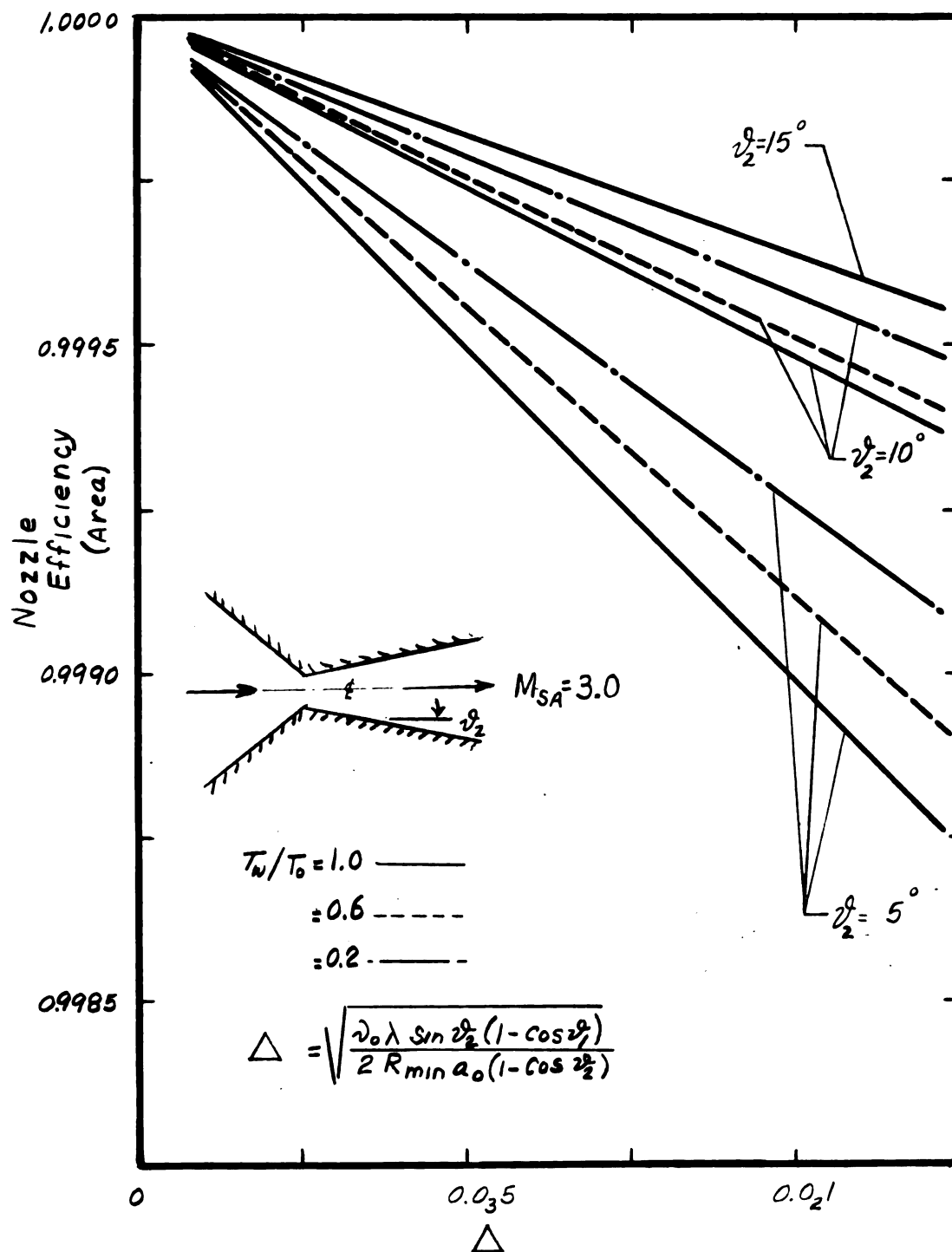
Fig. 10. Variation of nozzle efficiency with parameter
for exit M_{SA} = 3.0.
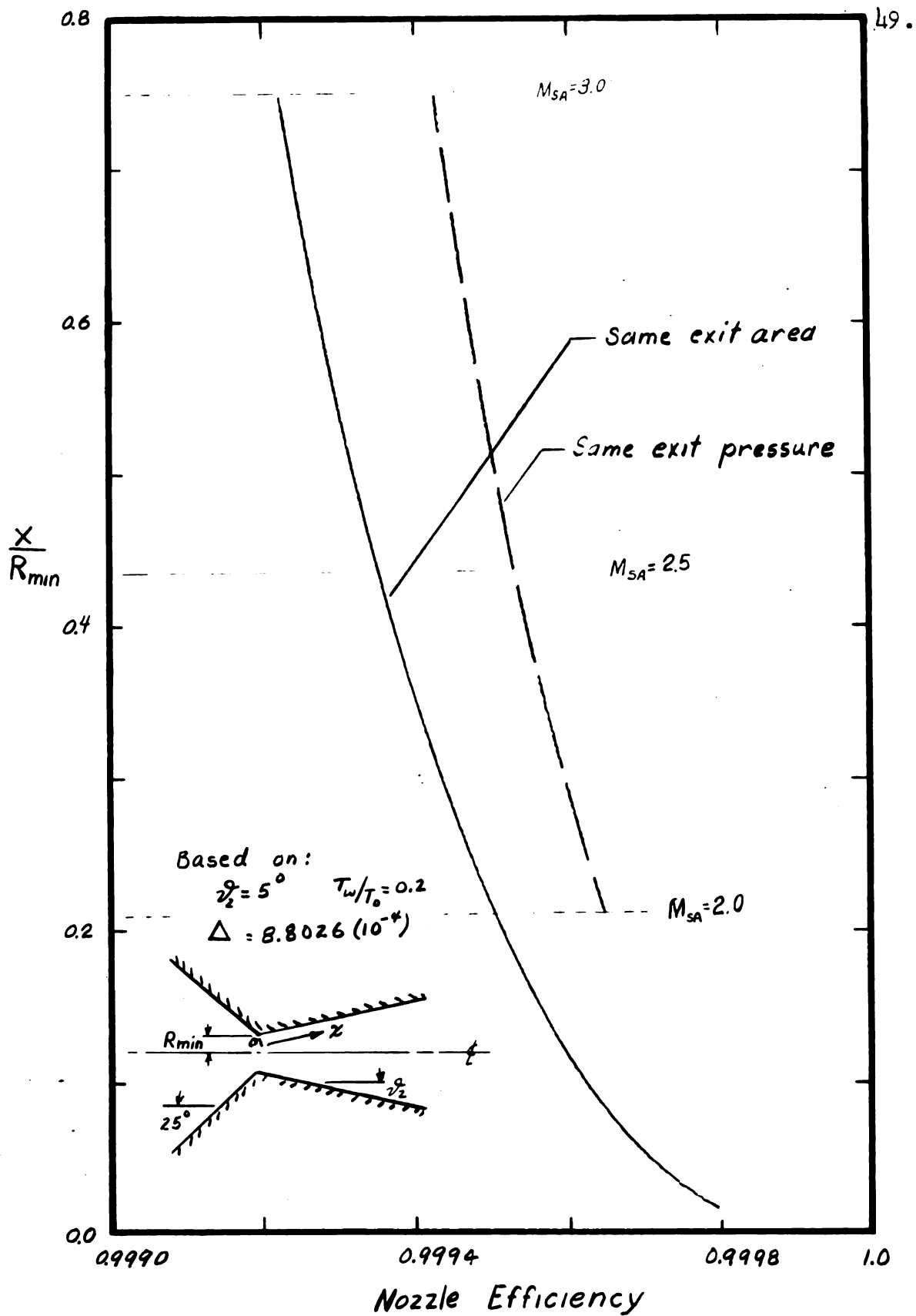
Fig. 11. Comparison of nozzle efficiency based on same exit area or pressure.

exit section for an actual and an ideal nozzle is convenient in thermo-dynamic studies since thermodynamic systems, the processes undergone, and resultant states are important. From the design standpoint, where physical equipment and effects of changes thereof are of primary inter-est, efficiencies based on area can be very useful. In the given ex-ample, comparison shows the pressure-based efficiency to be higher, and by about 30% of the remaining change from area-based efficiency to 100%. The pressure-based efficiency was expected to be higher because, using a given area, when frictional pressure drop occurs the exhaust pressure would not be reached in the fluid at exit section, and further expansion to this slightly lower pressure would allow M to be slightly larger in the corresponding pressure-based value.

The effects of skin friction and heat transfer as demonstrated in the change of nozzle efficiency appear quite small. However, it is well to restate that other phenomena known to occur under certain circumstances and difficult to evaluate analytically and experiment-ally, were not included.

The calculated data would say that for (1) a $M = 3$ nozzle with 30-inch diameter, stagnation pressure of 600 psia, stagnation tempera-ture of 3600°R and exhaust angle (θ_2) of 5°, the nozzle efficiency based on area is 0.9998 or (2) a $M = 3$ nozzle with 6-inch diameter, stagnation pressure of 10 psia, stagnation temperature of 4200°R, and exhaust angle of 5°, the efficiency is in the order of 0.997.

These values would be the estimate of efficiency of a nozzle with gas of $Pr = 1$ expanding with

1. smooth walls such that surface irregularities do not

   cause a disturbance in the flow to promote transition

   from laminar to turbulent boundary layer

2. exit pressure identical to exhaust regions

3. no discontinuities in the flow due to shocks

4. wall cooling to retain laminar layer

5. straight walls of large radius such that boundary layer

   thickness of fluid was negligible.

Shapiro[1] states "well-designed nozzles with straight axes . . . .

operated at design pressure ratios and at high Reynolds numbers, . . .

have efficiencies for 94-99 per cent, and even higher for sizable wind

tunnel nozzles."

The author believes that the values obtained of nozzle efficiency

including skin fricition and heat transfer effects are reasonable, and

if the effect of boundary thickness on area available for flow is in-

cluded, the combined analysis should constitute a reasonable approach

to predicting nozzle efficiencies of the given type. One author[2]

measured a linear growth of a laminar layer in supersonic wind tunnel

at an average of $0.7°$. Such growth could cause appreciable area change

and affect a change in efficiencies as much as one per cent.

[1]Shapiro, Ascher. The Dynamics and Thermodynamics of Compressible Fluid Flow, Vols. I and II. First Ed., New York: The Ronald Press Company, 1953, p. 99.

[2]McLellan, Charles, Thomas William, Ivan Beckwith. Investigation of the Flow Through a Single Stage Two-Dimensional Nozzle in the Langley Eleven Inch Hypersonic Tunnel. NACA TV 2223, 1951.

Extension of these results may not be made directly to a gas with Pr $\neq$ 1, e.g., air which has a Pr $\cong$ .75. However, a number of investigators have found that variation of Prandtl number has negligible effect on skin friction coefficients, and recently, methods have been used to modify Nusselt number (dimensionless heat transfer expression) for Prandtl number variation. Such modification in the given method would necessarily start with Equation (99).

CONCLUSIONS

This investigation dealt with the flow of compressible gas ($Pr = 1$) through a converging-diverging nozzle of large radius and straight walls of constant temperature.

The conclusions drawn on the basis of results obtained were:

1. The heat transfer effects relative to skin friction effects were dominant in magnitude in the subsonic region, and in the case of considerable cooling ($T_w /T_o = 0.2$) this effect extended into the supersonic region.

2. Skin friction effects were very dominant in supersonic region, to the point that heat energy losses may be considered negligible. If cooling at walls occur, however, the effects on boundary layer development must be considered in order to establish velocity gradients and hence skin friction effects.

3. Effects of skin friction and heat transfer on nozzle efficiency were small, resulting in a difference from 100 per cent of between 0.2 of one per cent to zero.

4. The effect of boundary layer thickness on nozzle efficiency should be included before expecting the results to accurately describe the best performance a well-designed nozzle might have.

APPENDIX

APPENDIX A

Transformation formulae used to change basic differential Equations (43), (44), (45), and (46), from cylindrical to space coordinates (x, y, ϑ).
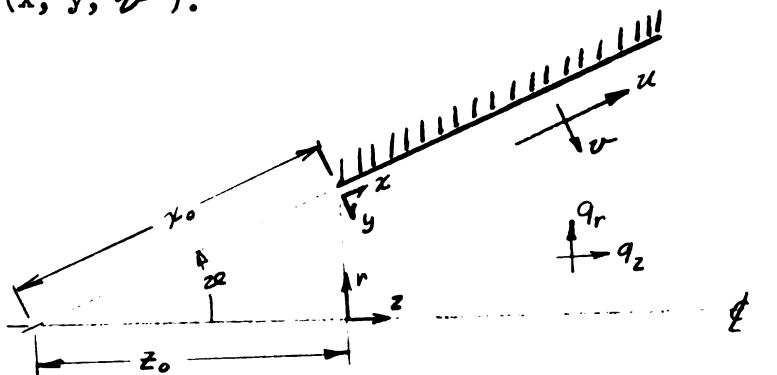
Velocity relations:

$$q_z = u \cos \vartheta + v \sin \vartheta$$

$$q_r = u \sin \vartheta - v \cos \vartheta$$

Space Coordinate relations:

$$x = - x_0 + (z + z_0) \cos \vartheta + r \sin \vartheta$$

$$y = (z + z_0) \sin \vartheta - r \cos \vartheta$$

Transformation Formulae:

$$\frac{\partial}{\partial r} = \frac{\partial}{\partial x} \frac{\partial x}{\partial r} + \frac{\partial}{\partial y} \frac{\partial y}{\partial r} , \quad \text{hence}$$

$$\frac{\partial}{\partial r} = \frac{\partial}{\partial x} \sin \vartheta - \frac{\partial}{\partial y} \cos \vartheta$$

$$\frac{\partial}{\partial z} = \frac{\partial}{\partial x} \frac{\partial x}{\partial z} + \frac{\partial}{\partial y} \frac{\partial y}{\partial z} , \quad \text{hence}$$

$$\frac{\partial}{\partial z} = \frac{\partial}{\partial x} \cos \vartheta + \frac{\partial}{\partial y} \sin \vartheta$$

APPENDIX B

Transformation formulae to change basic differential Equations (48), (49), and (50) into two-dimensional form using Mangler Transformation.

Mangler Transformations based on $R \cong r$ where $R = R(x)$:

$$x' = L \int_0^{x/L} \frac{R^2}{L^2} \, d\,(x/L)$$

$$y' = \frac{R}{L} y$$

Defining:

$$\frac{\partial \psi}{\partial y} = \rho uR \qquad \frac{\partial \psi}{\partial x} = -\rho Rv$$

$$\frac{\partial \psi'}{\partial y'} = \rho' u' \qquad \frac{\partial \psi'}{\partial x'} = -\rho' v'$$

$$p' = p \qquad\qquad h' = h$$

$$L = \text{fixed reference length}$$

Resultant Transformation Formulae

$$\frac{\partial}{\partial x} = \frac{R^2}{L^2} \frac{\partial}{\partial x'} + \frac{y'}{R} \frac{dR}{dx} \frac{\partial}{\partial y'} \qquad\qquad \frac{dx'}{dx} = \frac{R^2}{L^2}$$

$$\frac{\partial}{\partial y} = \frac{R}{L} \frac{\partial}{\partial y'} \qquad\qquad \frac{dy'}{dy} = \frac{R}{L}$$

$$\frac{dy'}{dx} = \frac{y'}{R} \frac{dR}{dx}$$

and some examples of formulae used:

$$\frac{\partial u}{\partial x} = \frac{R^2}{L^2} \frac{\partial u'}{\partial x'} + \frac{y'}{R} \frac{dR}{dx} \frac{\partial u'}{\partial y'}$$

$$\frac{\partial u}{\partial y} = \frac{R}{L} \frac{\partial u'}{\partial y'}$$

$$\frac{\partial p}{\partial x} = \frac{R^2}{L^2} \frac{\partial p'}{\partial x'}$$

$$\frac{\partial}{\partial y}\left(\mu \frac{R}{L} \frac{\partial u}{\partial y}\right) = \frac{R^2}{L^2}\left[\frac{\partial}{\partial y'}\left(\mu' \frac{\partial u'}{\partial y'}\right)\right]$$

Relation of u' to u and v' to v:

$$u' = u$$

$$v' = \frac{L}{R}\left(v + \frac{y}{R}\frac{dR}{dx} u\right)$$

Transformation formulae using modified Stewartson expressions to change two-dimensional Equations (56), (57), and (58) to essentially incompressible form.

Stream functions used in the two coordinate systems:

In x', y' system:

$$\frac{\partial \psi'}{\partial y'} = \frac{\rho' u'}{\rho_0'} \quad , \quad \frac{\partial \psi'}{\partial x'} = -\frac{\rho' v'}{\rho_0'}$$

In x'', y'' system:

$$\frac{\partial \psi''}{\partial y''} = u'' \quad , \quad \frac{\partial \psi''}{\partial x''} = -v$$

Transformation formulae:

$$\left(\frac{\partial}{\partial x'}\right)_{y'} = \left(\frac{\partial}{\partial x''}\right)_{y''}\left(\frac{\lambda\, a_e p_e}{P_0 a_0}\right) + \left(\frac{\partial}{\partial y''}\right)_{x''}\left(\frac{\partial y''}{\partial x'}\right)_{y'}$$

$$\left(\frac{\partial}{\partial y'}\right)_{x'} = \left(\frac{\partial}{\partial y''}\right)_{x''}\left(\frac{a_e\, \rho}{a_0\, \rho_0}\right)$$

The transformations were made assuming:

1. λ = constant, since wall temperature was constant.

2. External potential flow, hence a_e and p_e were dependent on x only, and Euler's equation $\left(\frac{1}{\rho_e}\frac{dp_e}{dx} = -u_e\frac{du_e}{dx}\right)$ was applicable to describe conditions at outer limit (δ) of boundary layer.

3. c_p and Pr as constant.

4. $p = p_e$ for any given value of x.

5. $p'' = p'$ and $T'' = T'$.

Relation of u' to u":

$$u' = \frac{\rho_0}{\rho} \frac{\partial \psi'}{\partial y'} = \frac{\rho_0}{\rho} \left(\frac{\partial \psi'}{\partial y''}\right)\left(\frac{\partial y''}{\partial y'}\right)_{x'} = \frac{\rho_0}{\rho} \frac{\partial \psi}{\partial y} \frac{\alpha_e}{\alpha_0} \frac{\rho}{\rho_0}$$

$$= \frac{\alpha_e}{\alpha_0} u''$$

APPENDIX D

Transformations and substitutions used to change Equations (65), (66), and (67) to a set of ordinary differential equations as a function of η only with $\beta = 2$ for $Pr = 1$:

Equations to be transformed

1. Continuity

$$\frac{\partial\left(\frac{\partial \psi''}{\partial y''}\right)}{\partial x''} - \frac{\partial\left(\frac{\partial \psi''}{\partial x''}\right)}{\partial y''} = 0$$

2. Energy

$$\frac{\partial \psi''}{\partial y''}\frac{\partial S}{\partial x''} - \frac{\partial \psi''}{\partial x''}\frac{\partial S}{\partial y''} = \nu_0 \cdot$$

$$\left[\frac{1}{Pr}\frac{\partial^2 S}{\partial y''^2} - \frac{1 - Pr}{Pr}\left(\frac{\frac{\gamma-1}{2}M_e^2}{1 + \frac{\gamma-1}{2}M_e^2}\right)\left(\frac{\partial^2\left(\frac{1}{u_e''}\frac{\partial \psi''}{\partial y''}\right)^2}{\partial y''^2}\right)\right]$$

3. Momentum

$$\frac{\partial \psi''}{\partial y''}\frac{\partial^2 \psi''}{\partial y''\partial x''} - \frac{\partial \psi''}{\partial x''}\frac{\partial^2 \psi''}{\partial y''^2} =$$

$$u_e''\frac{\partial u_e}{\partial x''}(1 + S) + \nu_0\frac{\partial^3 \psi''}{\partial y''^3}$$

Transformations:

1. $\psi'' = f(\eta)\sqrt{\frac{2 u_e'' \nu_0 L}{K_1}}$ with $\frac{\partial \psi''}{\partial y''} = u''$

2. $S = S(\eta)$ $\frac{\partial \psi''}{\partial x''} = -v''$

3. $y'' = \eta\sqrt{\frac{2 \nu_0 L}{K_1 u_e''}}$

Useful substitutions:

$$\left(\frac{\partial \psi''}{\partial \eta}\right)_{x''} = \sqrt{\frac{2\, u_e''\, \nu_o L}{K_1}} \; \frac{\partial f}{\partial \eta}$$

$$\left(\frac{\partial \eta}{\partial y''}\right)_{x''} = \sqrt{\frac{K_1 u_e''}{2\, \nu_o L}}$$

$$\left(\frac{\partial \psi''}{\partial y''}\right)_{x''} = \left(\frac{\partial \psi''}{\partial \eta}\right)_{x''} \left(\frac{\partial \eta}{\partial y''}\right)_{x''} = u_e'' \, \frac{\partial f}{\partial \eta}$$

$$\text{Note: } \frac{u''}{u_e''} = \frac{\partial f}{\partial \eta}$$

$$\left(\frac{\partial \left(\frac{\partial \psi''}{\partial y''}\right)_{x''}}{\partial x''}\right)_{\eta} = \left(\frac{\partial \left(c_1 e^{\frac{K_1 x''}{L}} \, \frac{\partial f}{\partial \eta}\right)}{\partial x''}\right)_{\eta} = \frac{u_e'' K_1}{L} \, \frac{\partial f}{\partial \eta}$$

$$\left(\frac{\partial \left(\frac{\partial \psi''}{\partial y''}\right)_{x''}}{\partial \eta}\right)_{x''} = u_e' \, \frac{\partial^2 f}{\partial \eta^2}$$

$$\left(\frac{\partial \eta}{\partial x''}\right)_{y''} = \frac{y''}{2} \sqrt{\frac{K_1 u_e''}{2 \nu_o L}} \; \frac{K_1}{L}$$

$$\left(\frac{\partial \left(\frac{\partial \psi''}{\partial y''}\right)_{x''}}{\partial x''}\right)_{y''} = \left(\frac{\partial \left(\frac{\partial \psi''}{\partial y''}\right)_{x''}}{\partial x''}\right)_{\eta} + $$

$$\left(\frac{\partial \left(\frac{\partial \psi''}{\partial y''}\right)_{x''}}{\partial \eta}\right)_{x''} \left(\frac{\partial \eta}{\partial x''}\right)_{y''} = $$

$$\frac{u_e'' K_1}{L} \frac{\partial f}{\partial \eta} + u_e'' \frac{\partial^2 f}{\partial \eta^2} \frac{y''}{2} \sqrt{\frac{K_1 u_e''}{2 \nu_0 L}} \frac{K_1}{L}$$

$$\left(\frac{\partial \left(\frac{\partial \psi''}{\partial y''} \right)_{x''}}{\partial y''} \right)_{x''} = \left(\frac{\partial \left(\frac{\partial \psi''}{\partial y} \right)_{x''}}{\partial \eta} \right)_{x''} \left(\frac{\partial \eta}{\partial y''} \right)_{x''} =$$

$$u_e'' \frac{\partial^2 f}{\partial \eta^2} \sqrt{\frac{K_1 u_e''}{2 \nu_0 L}}$$

$$\left(\frac{\partial^3 \psi''}{\partial y''^3} \right)_{x''} = u_e'' \frac{\partial^3 f}{\partial \eta^3} \sqrt{\frac{K_1 u_e''}{2 \nu_0 L}} \cdot \sqrt{\frac{K_1 u_e''}{2 \nu_0 L}} =$$

$$\frac{\left(u_e'' \right)^2 K_1}{2 \nu_0 L} \frac{\partial^3 f}{\partial \eta^3}$$

$$\left(\frac{\partial \psi''}{\partial x''} \right)_\eta = \frac{f}{2} \frac{K_1}{L} \frac{y''}{\eta} u_e''$$

$$\left(\frac{\partial \psi''}{\partial x''} \right)_{y''} = \left(\frac{\partial \psi''}{\partial x''} \right)_\eta + \left(\frac{\partial \psi''}{\partial \eta} \right)_{x''} \left(\frac{\partial \eta}{\partial x''} \right)_{y''} =$$

$$\frac{f}{2} \frac{K_1}{L} \sqrt{\frac{2 \nu_0 L}{K_1 u_e''}} u_e'' + \frac{\partial f}{\partial \eta} \frac{K_1}{L} \frac{y''}{2} u_e''$$

$$\left(\frac{\partial\left(\frac{\partial\psi''}{\partial x''}\right)_{y''}}{\partial y''}\right)_{x''} = \left(\frac{\partial\left(\frac{\partial\psi''}{\partial x''}\right)_{y''}}{\partial\eta}\right)_{x''}\left(\frac{\partial\eta}{\partial y''}\right)_{x''} =$$

$$\left[\frac{\partial f}{\partial\eta}\ \frac{K_1}{2L}\ \sqrt{\frac{2\nu_oL}{K_1\ u_e''}}\ u_e'' + \frac{\partial^2 f}{\partial\eta^2}\ \frac{y''}{2}u_e'' + \frac{\partial f}{\partial\eta}\ \frac{K_1}{2L}u_e''\cdot\right.$$

$$\left.\sqrt{\frac{2\nu_oL}{K_1 u_e''}}\right]\ \sqrt{\frac{K_1 u_e''}{2\nu_oL}}\ \frac{K_1}{L}$$

$$\left(\frac{\partial s}{\partial x''}\right)_{y''} = \left(\frac{\partial s}{\partial\eta}\right)_{x''}\left(\frac{\partial\eta}{\partial x''}\right)_{y''} = \frac{\partial s}{\partial\eta}\frac{y''}{2}\ \sqrt{\frac{K_1 u_e''}{2\nu_oL}}\ \frac{K_1}{L}$$

$$\left(\frac{\partial s}{\partial y''}\right)_{x''} = \left(\frac{\partial s}{\partial\eta}\right)_{x''}\left(\frac{\partial\eta}{\partial y''}\right)_{x''} = \frac{\partial s}{\partial\eta}\ \sqrt{\frac{K_1 u_e''}{2\nu_oL}}$$

$$\left(\frac{\partial\left(\frac{\partial s}{\partial y''}\right)_{x''}}{\partial y''}\right)_{x''} = \frac{\partial^2 s}{\partial\eta^2}\ \frac{K_1 u_e''}{2\nu_oL}$$

APPENDIX E

TABLE I

Calculated Data Including Data of K_1 for $M_{SA} > 0.0010$

Based on $\not{\theta}_1 = 25°$ $L = r_{pl}*$

$\not{\theta}_2 = 15°$ $\dfrac{x}{L} = 0$ at $M_{SA} = 0.001$

$\gamma = 1.4$

where $\pi_2 = \dfrac{\ln M_{SA}/M_{\frac{x}{L}=0}}{\pi_1}$, $\pi_1 = \displaystyle\int_0^{x/L} \left(\frac{r_e}{r_o}\right)^{k_0} \frac{A}{A^*}\, d\!\left(\frac{x}{L}\right)$

(1) M_{SA}	(2) $\ln \dfrac{M_{SA}}{M_{\frac{x}{L}=0}}$	(3) $\dfrac{T_{SA}}{T_o}$	(4) $\dfrac{A}{A^*}$	(5) $\dfrac{x}{L}$	(6) π_1	(7) π_2
0.0010	0.00000000	0.99999980	578.70405	0.00000	0.00000	0.000000000
0.0012	0.18232155	0.99999971	482.2535	2.09600		
0.0014	0.33647222	0.99999961	413.3603	3.72502	1835.11241	$0.0_3183352$
0.0016	0.47000344	0.99999949	361.6904	5.03812		
0.0018	0.58778648	0.99999935	321.5027	6.12578	2999.82137	$0.0_3195940$
0.0020	0.69314718	0.99999920	289.3525	7.04591		
0.0025	0.91629072	0.99999875	231.4823	8.84173		
0.0030	1.09861229	0.99999820	192.9023	10.16735	3747.41508	$0.0_3293165$
0.0035	1.25276	0.99999755	165.3451	11.19762	3931.7779	$0.0_3318624$
0.0040	1.38629436	0.99999680	144.6773	11.92809	4060.41404	$0.0_3341426$
0.0045	1.50408	0.99999595	128.6024	12.71598		
0.0050	1.60943791	0.99999500	115.7425	13.29791	4225.41533	$0.0_3380894$
0.0055	1.70475	0.99999395	105.2208	13.79855		
0.0060	1.79175947	0.99999280	96.4499	14.23524	4324.72571	$0.0_3344305$
0.0065	1.87180	0.99999155	89.0338	14.62050		
0.0070	1.94591015	0.9999902	82.6744	14.96373		

0.0075	2.01490307	0.9999887	77.1631	15.26192		
0.0080	2.07944154	0.9999872	72.3407	15.55094		
0.0085	2.14006617	0.9999855	68.0818	15.80486		
0.0090	2.19722458	0.9999838	64.3035	16.03733	4435.38629	$0.0_3468842$
0.0095	2.25129180	0.9999819	60.9194	16.25119		
0.0100	2.30258509	0.999980	57.8738	16.44879	4493.5930	$0.0_3512425$
0.015	2.70805020	0.9999775	38.5855	17.84455	4588.5793	$0.0_3652864$
0.020	2.99573227	0.99992	28.9421	18.67650		
0.025	3.21887582	0.9998750	23.1568	19.24412		
0.030	3.40119738	0.99982	19.300	19.66307		
0.040	3.68887945	0.99968	14.482	20.25077		
0.050	3.91202300	0.999500	11.5915	20.65165	4625.0020	$0.0_3845850$
0.060	4.09434456	0.99928	9.6659	20.94727		
0.070	4.24849524	0.99902	8.2915	21.17678		
0.080	4.38202663	0.99872	7.2616	21.37267		
0.090	4.49980967	0.99838	6.4613	21.51436	4634.9597	$0.0_3970841$
0.100	4.60517018	0.99800	5.8218	21.64347	4635.0022	$0.0_3993416$
0.300	5.70378247	0.98232	2.0351	22.50778	4639.7581	$0.0_21190237$
0.500	6.21460810	0.95238	1.3398	22.89877	4639.8610	$0.0_2133942$
0.700	6.55108033	0.91075	1.09437	23.01017	4639.8907	$0.0_21411913$
1.000	6.90775528	0.83333	1.00000	23.05627	4640.0075	$0.0_21488985$
1.500	7.31322039	0.68965	1.1762	23.19644		$0.0_21576146$
2.000	7.60090246	0.55556	1.6875	23.53974		$0.0_21638122$
2.500	7.82404601	0.44444	2.6367	24.01367		0.0_216862
3.000	8.00636757	0.35714	4.2346	24.81032	4640.1392	$0.0_21725558$
3.600	8.18868912	0.27840	7.4501	25.92411	4640.2003	$0.0_21764727$
4.000	8.29404964	0.23810	10.719	26.82700	4640.2356	$0.0_21787419$

Note: 0.0_35 means 0.0005

TABLE II

Calculated Data for $0.100 \leq M_{SA} \leq 1.00$

Based on: $\theta_2 = 25°$, $\gamma = 1.4$, $L = r_{pl}*$, and $\dfrac{x}{L} = 0$ at $M = 0.001$

(1) M_{SA}	(2) $\ln \dfrac{M_{SA}}{\frac{M_x}{L} = 0}$	(3) $\dfrac{A}{A*}$	(4) $\dfrac{T_{SA}}{T_o}$	(5) $\dfrac{x}{L}$	(6) $\displaystyle\int_0^{x/L} \left(\dfrac{T_e}{T_o}\right)^4 \dfrac{A}{A*}\, d\left(\dfrac{x}{L}\right)$
0.100	4.60517018	5.8218	0.998004	21.64342	4635.002
0.120	4.78749174	4.8643	0.997128	21.85076	4636.099
0.140	4.94164242	4.1824	0.996095	22.01118	4636.815
0.160	5.01063529	3.6727	0.994906	22.13985	4637.311
0.180	5.19295685	3.2779	0.993562	22.24578	4637.670
0.200	5.29831737	2.9635	0.992063	22.33479	4637.940
0.220	5.39362755	2.7076	0.990412	22.41080	4638.147
0.240	5.48063892	2.4956	0.988480	22.47653	4638.311
0.260	5.56068163	2.3173	0.986660	22.53401	4638.443
0.280	5.63478960	2.1656	0.984562	22.58468	4638.550
0.300	5.70378247	2.0351	0.982316	22.62970	4638.638
0.350	5.85793315	1.7780	0.976086	22.72285	4638.801
0.400	5.99146455	1.5901	0.968992	22.79527	4638.910
0.450	6.10924758	1.4487	0.961076	22.85265	4638.986
0.500	6.21460810	1.3398	0.952381	22.89877	4639.039
0.550	6.30991828	1.2550	0.942951	22.93600	
0.600	6.39692965	1.1882	0.932844	22.96622	
0.650	6.47697236	1.1356	0.922084	22.99063	
0.700	6.55108033	1.0944	0.910745	23.01017	
0.750	6.62007320	1.0624	0.898876	23.02554	

0.800	6.68461173	1.0382	0.886525	23.03734
0.850	6.74523635	1.0207	0.873744	23.04597
0.900	6.80239476	1.0089	0.860585	23.05183
0.950	6.85646198	1.0022	0.847099	23.05517
1.000	6.90775528	1.0000	0.833333	23.05627

TABLE II (cont.)

(1) M_{SA}	(7) $\dfrac{\ln M_{SA}/M_{x=0}}{M_{SA}\ \text{(col.6)}}$	(8) $\dfrac{1}{1+\frac{\tau}{2}M_{SA}^2}\sqrt{\text{(col 7)}}$	(9) $\dfrac{\delta M_{SA}^2}{1+\frac{\tau}{2}M_{SA}^4}\sqrt{\text{col 7}}$	(10) $\dfrac{1+\delta M_{SA}^4}{1+\frac{\tau}{2}M_{SA}^3}\sqrt{\text{(col 7)}}$	(11) $(\overline{\text{Col. 8}})\ \Delta x$
0.100	0.02939564	0.099478723	0.00139270	0.10087143	
0.120	0.02860562	0.09250005	0.00186480	0.09436485	0.0199024
0.140	0.02761243	0.08690853	0.00238477	0.08929330	0.0143904
0.160	0.02675315	0.08175894	0.00293024	0.08468918	0.0108512
0.180	0.02622074	0.07836884	0.00355481	0.08192365	0.00854472
0.200	0.02571193	0.07497745	0.00419873	0.07917619	0.00682468
0.220	0.02528584	0.07200670	0.00487917	0.07688587	0.00558613
0.240	0.02492335	0.06935826	0.00559305	0.07495131	0.00464596
0.260	0.02461086	0.06699748	0.00634064	0.07333812	0.00391886
0.280	0.02438848	0.06485027	0.00711796	0.07196823	0.00334036
0.300	0.02409875	0.06288945	0.00792407	0.07081352	0.00283040
0.350	0.02360803	0.05863044	0.01005512	0.06868556	0.00565979
0.400	0.02322892	0.05506159	0.01233380	0.06739539	0.00411110
0.450	0.02292652	0.05199164	0.01473963	0.06673127	0.00307136
0.500	0.02267926	0.04929673	0.01725385	0.06655058	0.00233571
0.550	0.02247307	0.04689292	0.01985915	0.06675207	0.00179057
0.600	0.02229824	0.04472050	0.02253913	0.06725963	0.00138428
0.650	0.02214800	0.04273537	0.02527797	0.06801334	0.00106740
0.700	0.02201739	0.04090648	0.02806185	0.06896832	0.00081716
0.750	0.02190273	0.03920924	0.03087728	0.07008652	0.00061569
0.800	0.02180120	0.03762246	0.03370972	0.07133218	0.00045331
0.850	0.02171062	0.03613770	0.03655328	0.07269098	0.00031828
0.900	0.02162928	0.03473691	0.03939165	0.07412857	0.00020770
0.950	0.02155579	0.03341255	0.04221676	0.07562931	0.00011380
1.000	0.02148906	0.03215697	0.04501976	0.07717673	0.00003606

TABLE II (cont.)

(1) M_{SA}	(12) $\sqrt{\sum \overline{Col. 8}} \, \Delta x$	(13) (Col. 9) Δx	(14) $\sum \overline{(Col. 9)} \, \Delta x$	(15) (Col. 10) Δx	(16) $\sqrt{\sum \overline{(Col. 10)}} \, \Delta x$
0.100	0.0199024	0.000337705	0.000337705	0.0202401	0.0202401
0.120	0.0342928	0.000340957	0.000678562	0.0147312	0.0349713
0.140	0.0451440	0.000341941	0.001020503	0.0111932	0.0461645
0.160	0.0536887	0.000343480	0.001363983	0.00882465	0.0549891
0.180	0.0605134	0.000345070	0.001709053	0.00716975	0.0621589
0.200	0.0660995	0.000345006	0.002054059	0.00593114	0.0680900
0.220	0.0707455	0.000344170	0.002398229	0.00499013	0.0730801
0.240	0.0746444	0.000342974	0.002741203	0.00426184	0.0773419
0.260	0.0780048	0.000340974	0.003082177	0.00368133	0.0810232
0.280					
0.300	0.0808352	0.000338596	0.003420773	0.00321402	0.0842372
0.350	0.0864950	0.000837380	0.004258153	0.00649717	0.0907344
0.400	0.0906061	0.000809583	0.005067736	0.00492069	0.0956551
0.450	0.0936775	0.000776736	0.005844472	0.00384809	0.0995032
0.500	0.0960132	0.000737770	0.006582242	0.00307348	0.1025767
0.550	0.0978038	0.000690858	0.007273100	0.00248143	0.1050581
0.600	0.0991881	0.000640638	0.007913738	0.00202492	0.1070830
0.650	0.1002555	0.000583608	0.008497346	0.00165101	0.1087340
0.700	0.1010727	0.000521131	0.009018477	0.00133831	0.1100723
0.750	0.1016884	0.000452947	0.009471424	0.00106864	0.1111409
0.800	0.1021417	0.000381063	0.009852487	0.00085797	0.1119989
0.850	0.1024600	0.000303185	0.010155672	0.00062146	0.1126204
0.900	0.1026677	0.000222519	0.010378191	0.00043018	0.1130506
0.950	0.1027815	0.000136286	0.010514477	0.00025009	0.1133007
1.000	0.1028176	0.000047980	0.010562457	0.00008404	0.1133847

APPENDIX E

TABLE III

Calculated Data for $M_{SA} \geq 1.00$

Based on $\vartheta_1 = 25°$ $L = r_{pl}*$

$\vartheta_2 = 5°$

$\gamma = 1.4$

$\dfrac{x}{L} = 0$ at $M = 0.001$

(1) M_{SA}	(2) $\ln \dfrac{M_{SA}}{M_{\frac{x}{L}=0}}$	(3) $\dfrac{A}{A*}$	(4) $\dfrac{T_{SA}}{T_o}$	(5) $\dfrac{x}{L}$	(6) $\displaystyle\int_0^{x/L} \left(\dfrac{T_e}{T_o}\right)^4 \dfrac{A}{A*}\, d(x/L)$
					4640.0
1.00	6.90775528	1.0000	0.83333	23.05627	
1.05	6.95654544	1.00202	0.81933	23.06128	
1.10	7.00306546	1.00793	0.80515	23.07584	
1.15	7.04751722	1.01746	0.79083	23.09940	
1.20	7.09007683	1.03044	0.77640	23.03123	
1.25	7.13089883	1.04676	0.76190	23.17095	
1.30	7.17011954	1.06631	0.74738	23.21815	
1.35	7.20785987	1.08904	0.73287	23.27246	
1.40	7.24422751	1.1149	0.71839	23.33359	
1.45	7.27931883	1.1440	0.70397	23.40153	
1.50	7.31322039	1.1762	0.68965	23.47571	
1.55	7.34601021	1.2115	0.67545	23.55585	
1.60	7.37775891	1.2502	0.66138	23.64243	
1.65	7.40853057	1.2922	0.64746	23.73482	
1.70	7.43838353	1.3376	0.63372	23.83307	
1.75	7.46737107	1.3865	0.62016	23.93698	

4640.0

1.80	7.49554194	1.4390	0.60680	24.04664
1.85	7.52294092	1.4952	0.59365	24.16172
1.90	7.54960916	1.5552	0.58072	24.28223
1.95	7.57558465	1.6193	0.56802	24.40851
2.00	7.60090246	1.6875	0.55556	24.54011
2.05	7.62559507	1.7600	0.54333	24.67711
2.10	7.64969262	1.8369	0.53135	24.81937
2.15	7.67322312	1.9185	0.51962	24.96729
2.20	7.69621264	2.0050	0.50813	25.12036
2.25	7.71868549	2.0964	0.49689	25.27870
2.30	7.74066440	2.1931	0.48591	25.44255
2.35	7.76217061	2.2953	0.47517	25.61180
2.40	7.78322402	2.4031	0.46468	25.78632
2.45	7.80384330	2.5168	0.45444	25.96619
2.50	7.82404601	2.6367	0.44444	26.15152
2.55	7.84384864	2.7630	0.43469	26.34226
2.60	7.86326672	2.8960	0.42517	26.53841
2.65	7.88231492	3.0359	0.41589	26.73996
2.70	7.90100705	3.1830	0.40684	26.94693
2.75	7.91935619	3.3376	0.39801	27.15940
2.80	7.93737469	3.5001	9.38941	27.37738
2.85	7.95507427	3.6707	0.38102	27.60102
2.90	7.97246601	3.8498	0.37286	27.83017
2.95	7.98956045	4.0376	0.36490	28.06482
3.00	8.00636757	4.2346	0.35714	28.30513

TABLE III (cont.)

(1)	(7)	(8)	(9)	(10)	(11)
M_{SA}	$\dfrac{\ln M_{SA}/M_{SA=u}}{M_{SA}}$ (Col 6)	$\dfrac{1}{1+\frac{\gamma-1}{2}M_{SA}^2}\sqrt{}$ (Col 7)	$\dfrac{\gamma M_{SA}^2}{1+\frac{\gamma-1}{2}M_{SA}^2}\sqrt{}$ (Col 7)	$\dfrac{1+\gamma M_{SA}^2}{1+\frac{\gamma-1}{2}M_{SA}^2}\sqrt{}$ (Col 7)	(Col. 8) Δx
1.00	0.0385883	0.03215697	0.04501976	0.07717673	0.00003606
1.05	0.0377870	0.03096002	0.04778679	0.07874681	0.00015811
1.10	0.0370415	0.02982396	0.05052179	0.08034575	0.00044251
1.15	0.0363421	0.02874042	0.05321289	0.08195331	0.00068989
1.20	0.0356842	0.02770521	0.05585370	0.08355891	0.00089833
1.25	0.0350638	0.02671511	0.05843930	0.08515444	0.00108079
1.30	0.0344772	0.02576756	0.06096605	0.08673361	0.00123859
1.35	0.0339217	0.02486020	0.06343308	0.08829100	0.00137480
1.40	0.0333943	0.02399013	0.06582892	0.08981905	0.00149311
1.45	0.0328929	0.02315561	0.06815854	0.09131415	0.00160154
1.50	0.0324153	0.02235521	0.07041891	0.09277412	0.00168799
1.55	0.0319595	0.02158704	0.07260801	0.09419505	0.00176077
1.60	0.0315241	0.02084941	0.07472429	0.09557369	0.00183707
1.65	0.0311075	0.02014043	0.07676525	0.09690568	0.00189353
1.70	0.0307083	0.01946046	0.07873702	0.09810748	0.00194540
1.75	0.0303253	0.01880654	0.08063304	0.09943958	0.00198816
1.80	0.0299575	0.01817821	0.08245636	0.1006346	0.00202787
1.85	0.0296039	0.01757436	0.08420754	0.1017819	0.00205720
1.90	0.0292635	0.01699390	0.08588717	0.1028811	0.00208291
1.95	0.0289355	0.01643594	0.08749673	0.1039327	0.00211076
2.00	0.0286192	0.01589956	0.08903754	0.1049371	0.00212767
2.05	0.0283140	0.01538385	0.09051088	0.1058947	0.00214291
2.10	0.0280190	0.01488790	0.09191789	0.1068058	0.00215323
2.15	0.0277339	0.01441109	0.09326137	0.1076725	0.00216695
2.20	0.0274579	0.01395218	0.09453997	0.1084922	0.00217078

69.

2.25	0.0271908	0.01351084	0.09575808	0.1092689	0.00217425
2.30	0.0269318	0.01308643	0.09691810	0.1100045	0.00217898
2.35	0.0266808	0.01267792	0.09801934	0.1106973	0.00218031
2.40	0.0264371	0.01228479	0.09906455	0.1113493	0.00217825
2.45	0.0262007	0.01190665	0.10005753	0.1119642	0.00217566
2.50	0.0259709	0.01154251	0.10099696	0.1125395	0.00217292
2.55	0.0257475	0.01119218	0.10188801	0.1130746	0.00216821
2.60	0.0255303	0.01085472	0.10272907	0.1135838	0.00216225
2.65	0.0253189	0.01052988	0.10352452	0.1140544	0.00215503
2.70	0.0251131	0.01021701	0.10427480	0.1144918	0.00214599
2.75	0.0249126	0.00991546	0.10497998	0.1148954	0.00213877
2.80	0.0247726	0.009625248	0.10564562	0.1152708	0.00212973
2.85	0.0245268	0.009345201	0.10626895	0.1156142	0.00212126
2.90	0.0243410	0.009075785	0.10685829	0.1159341	0.00211058
2.95	0.0241597	0.008815875	0.10740821	0.1162241	0.00209914
3.00	0.0239827	0.008565181	0.10792128	0.1164865	0.00208842

TABLE III (cont.)

(1)	(12)	(13)	(14)	(15)	(16)
M_{SA}	$\sum(\text{Col. } 8)\,\Delta x$	$(\text{Col. } 9)\,\Delta x$	$\sum(\text{Col. } 9)\,\Delta x$	$(\text{Col. } 10)\,\Delta x$	$\sum(\text{Col. } 10)\,\Delta x$
1.00	0.1028176	0.00004798	0.01056246	0.00008404	0.1133847
1.05	0.1029757	0.00023248	0.01079494	0.00039059	0.1137753
1.10	0.1034182	0.00071569	0.01151063	0.00115819	0.1149335
1.15	0.1041081	0.00122199	0.01273262	0.00191188	0.1168454
1.20	0.1050064	0.00173580	0.01446842	0.00263413	0.1194795
1.25	0.1060872	0.00226986	0.01673828	0.00335065	0.1228301
1.30	0.1073258	0.00281797	0.01955625	0.00405656	0.1268867
1.35	0.1087006	0.00337806	0.02293431	0.00475279	0.1316395
1.40	0.1101937	0.00395089	0.02688520	0.00544393	0.1370834
1.45	0.1117952	0.00455155	0.03143675	0.00615309	0.1432365
1.50	0.1134832	0.00513934	0.03657659	0.00682783	0.1500643
1.55	0.1152440	0.00573109	0.04230768	0.00749185	0.1575561
1.60	0.1170811	0.00637758	0.04868526	0.00821509	0.1657712
1.65	0.1189746	0.00699801	0.05568327	0.00889158	0.1746628
1.70	0.1209203	0.00763905	0.06332232	0.00958444	0.1842472
1.75	0.1229082	0.00828007	0.07160239	0.01026823	0.1945154
1.80	0.1249361	0.00894219	0.08054458	0.01097007	0.2054855
1.85	0.1260033	0.00958984	0.09013442	0.01164704	0.2171325
1.90	0.1290762	0.01024906	0.10038348	0.01233197	0.2294645
1.95	0.1311870	0.01094746	0.11133094	0.01305822	1.2425227
2.00	0.1333147	0.01161595	0.12294689	0.01374363	0.2562663
2.05	0.1354576	0.01229907	0.13524596	0.01444191	0.2707082
2.10	0.1376108	0.01297616	0.14822212	0.01512938	0.2858376
2.15	0.1397778	0.01369586	0.16191798	0.01586282	0.3017004
2.20	0.1419486	0.01437338	0.17629136	0.01654416	0.3182445
2.25	0.1441229	0.01506589	0.19135725	0.01724014	0.3354847

2.30	0.1463019	0.01578499	0.20714224	0.01796397	0.3534487
2.35	0.1484822	0.01649658	0.22363882	0.01867689	0.3721256
2.40	0.1506605	0.01719754	0.24083636	0.01937579	0.3915016
2.45	0.1528362	0.01790804	0.25874440	0.02008369	0.4115853
2.50	0.1550091	0.01873071	0.27737511	0.02080363	0.4323889
2.55	0.1571773	0.01934914	0.29672425	0.02151681	0.4539057
2.60	0.1593396	0.02006782	0.31679207	0.02229522	0.4762009
2.65	0.1614946	0.02078520	0.33757727	0.02294024	0.4991411
2.70	0.1636416	0.02150411	0.35908138	0.02365110	0.5227922
2.75	0.1657804	0.02223018	0.38131156	0.02436895	0.5471612
2.80	0.1679101	0.02295608	0.41426764	0.02508581	0.5722470
2.85	0.1700314	0.02369629	0.42796393	0.02581756	0.5980646
2.90	0.1721420	0.02444905	0.45238298	0.02652964	0.6245942
2.95	0.1742411	0.02513882	0.47752180	0.02723796	0.6518322
3.00	0.1763295	0.02587291	0.50339471	0.02796134	0.6797935

TABLE III (cont.)

(1) M_{SA}	(12) $\sum$(Col. 8) Δx	(13) (Col. 9) Δx	(14) $\sum$(Col. 9) Δx	(15) (Col. 10) Δx	(16) $\sum$(Col. 10) Δx
1.00	0.1028176	0.00004798	0.01056246	0.00008404	0.1133847
1.05	0.1029757	0.00023248	0.01079494	0.00039059	0.1137753
1.10	0.1034182	0.00071569	0.01151063	0.00115819	0.1149335
1.15	0.1041081	0.00122199	0.01273262	0.00191188	0.1168454
1.20	0.1050064	0.00173580	0.01446842	0.00263413	0.1194795
1.25	0.1060872	0.00226986	0.01673828	0.00335065	0.1228301
1.30	0.1073258	0.00281797	0.01955625	0.00405656	0.1268867
1.35	0.1087006	0.00337806	0.02293431	0.00475279	0.1316395
1.40	0.1101937	0.00395089	0.02688520	0.00544393	0.1370834
1.45	0.1117952	0.00455155	0.03143675	0.00615309	0.1432365
1.50	0.1134832	0.00513984	0.03657659	0.00682783	0.1500643
1.55	0.1152440	0.00573109	0.04230768	0.00749185	0.1575561
1.60	0.1170811	0.00637758	0.04868526	0.00821509	0.1657712
1.65	0.1189746	0.00699801	0.05568327	0.00889158	0.1746528
1.70	0.1209200	0.00763905	0.06332232	0.00958444	0.1842472
1.75	0.1229082	0.00828007	0.07160239	0.01026823	0.1945154
1.80	0.1249361	0.00894219	0.08054458	0.01097007	0.2054855
1.85	0.1260033	0.00958984	0.09013442	0.01164704	0.2171325
1.90	0.1290762	0.01024906	0.10038348	0.01233197	0.2294645
1.95	0.1311870	0.01094746	0.11133094	0.01305822	1.2425227
2.00	0.1333147	0.01161595	0.12294689	0.01374363	0.2562663
2.05	0.1354576	0.01229907	0.13524596	0.01444191	0.2707082
2.10	0.1376108	0.01297616	0.14822212	0.01512938	0.2858376
2.15	0.1397778	0.01369586	0.16191798	0.01586282	0.3017004
2.20	0.1419486	0.01437338	0.17629136	0.01654416	0.3182445
2.25	0.1441229	0.01506589	0.19135725	0.01724014	0.3354847

2.30	0.1463019	0.01578499	0.20714224	0.01796397	0.3534487
2.35	0.1484822	0.01649658	0.22363882	0.01867689	0.3721256
2.40	0.1506605	0.01719754	0.24083636	0.01937579	0.3915016
2.45	0.1528362	0.01790804	0.25874440	0.02008369	0.4115853
2.50	0.1550091	0.01873071	0.27737511	0.02080363	0.4323889
2.55	0.1571773	0.01934914	0.29672425	0.02151681	0.4539057
2.60	0.1593396	0.02006782	0.31679207	0.02229522	0.4762009
2.65	0.1614946	0.02078520	0.33757727	0.02294024	0.4994411
2.70	0.1636416	0.02150411	0.35908138	0.02365110	0.5227922
2.75	0.1657804	0.02223018	0.38131156	0.02436895	0.5471612
2.80	0.1679101	0.02295608	0.41426764	0.02508581	0.5722470
2.85	0.1700314	0.02369629	0.42796393	0.02581756	0.5980646
2.90	0.1721420	0.02441905	0.45238298	0.02652964	0.6245942
2.95	0.1742411	0.02513882	0.47752180	0.02723796	0.6518322
3.00	0.1763295	0.02587291	0.50339471	0.02796134	0.6797935

TABLE IV

Additional Calculated Data for $1.0 \leq M \leq 3.0$

Based on $\theta_1 = 25°$, $\gamma = 1.4$, $L = r_{pl}*$, $\dfrac{x}{L} = 0$ at $M = 0.001$

where

$$\Delta = \sqrt{\dfrac{\mathcal{D}_0 \lambda \sin\theta_2 \,(1 - \cos\theta)}{2a_0\, R_{min}\,(1 - \cos\theta_2)}} \qquad ; \qquad A = \dfrac{\sin^2\theta}{(1 - \cos\theta)\,\sin\theta_1}$$

(1)	(2)	(3)	(4)	(5)	(6)	(7)
$\dfrac{T_w}{T_0}$	θ_2	M_{SA}	$\dfrac{(A)(\Delta)}{2}\left(\dfrac{\partial s}{\partial\eta}\right)_w \begin{bmatrix} col\,16 \\ Table\,III \end{bmatrix}$	$(A)(\Delta)\left(\dfrac{\partial f}{\partial\eta}\right)_w \begin{bmatrix} col\,14 \\ Table\,III \end{bmatrix}$	$\ln\left[\dfrac{1+\frac{\gamma-1}{2}M_{SA}^2}{1+\frac{\gamma-1}{2}M^2}\right]^{3.0}\dfrac{M}{M_{SA}}$	$\ln\dfrac{T_{02}}{T_{01}}$
1.0	15°	1.00			$0.0_4211153440$	
	15°	1.50			$0.0_4390380820$	
	15°	2.00			$0.0_4985424749$	
	15°	2.50			$0.0_4204935993$	
	15°	3.00			$0.0_4360653378$	
	10°	1.00			$0.0_4211153440$	
	10°	1.50			$0.0_4482144287$	
	10°	2.00			$0.0_4381886655$	
	10°	2.50			$0.0_3299053999$	
	10°	3.00			$0.0_3534449811$	
	5°	1.00			$0.0_4211153440$	
	5°	1.50			$0.0_4755721882$	
	5°	2.00			$0.0_4256376022$	
	5°	2.50			$0.0_3579649342$	
	5°	3.00			$0.0_2105278900$	

$\Delta = 2.6270 \times 10^{-4}$

θ = 0.5, ∇ = 2.9341 × 10⁻⁴

15°	1.00	$-0.0_417287820$	$0.0_418633560$	$0.0_5134574$	$-0.0_431353299$
15°	1.50	$-0.0_419215207$	$0.0_434449762$	$0.0_4152346$	$-0.0_432474192$
15°	2.00	$-0.0_424795599$	$0.0_486960577$	$0.0_46216498$	$-0.0_434558299$
15°	2.50	$-0.0_434050445$	$0.0_318084889$	$0.0_31467987$	$-0.0_436838168$
15°	3.00	$-0.0_447046976$	$0.0_331826452$	$0.0_32712175$	$-0.0_439079791$
10°	1.00	$-0.0_417287820$	$0.0_418633560$	$0.0_48134574$	$-0.0_431353299$
10°	1.50	$-0.0_420202175$	$0.0_425547445$	$0.0_42234527$	$-0.0_433048137$
10°	2.00	$-0.0_428640152$	$0.0_442191494$	$0.0_49330479$	$-0.0_436199462$
10°	2.50	$-0.0_442633342$	$0.0_326390482$	$0.0_42212715$	$-0.0_439646764$
10°	3.00	$-0.0_462284823$	$0.0_347167612$	$0.0_34093913$	$-0.0_443033613$
5°	1.00	$-0.0_417287820$	$0.0_418633560$	$0.0_40134574$	$-0.0_431353299$
5°	1.50	$-0.0_4231440481$	$0.0_466689853$	$0.0_44354577$	$-0.0_434759036$
5°	2.00	$-0.0_440100282$	$0.0_322624300$	$0.0_31861427$	$-0.0_441091627$
5°	2.50	$-0.0_468219998$	$0.0_351152057$	$0.0_3443006$	$-0.0_448019079$
5°	3.00	$-0.0_310772065$	$0.0_392904997$	$0.0_38213293$	$-0.0_454827104$

θ = 0.2, ∇ = 3.5725 × 10⁻⁴

15°	1.00	$-0.0_439567288$	$0.0_416135878$	$-0.0_42343141$	$-0.0_471759482$
15°	1.50	$-0.0_443978528$	$0.0_429832035$	$-0.0_41414649$	$-0.0_474324887$
15°	2.00	$-0.0_456750455$	$0.0_475304168$	$+0.0_41855371$	$-0.0_479094814$
15°	2.50	$-0.0_477931473$	$0.0_315660746$	$+0.0_47867598$	$-0.0_484312786$
15°	3.00	$-0.0_310767752$	$0.0_327560355$	$+0.0_31679260$	$-0.0_489440932$
10°	1.00	$-0.0_439567288$	$0.0_416135878$	$-0.0_42343141$	$-0.0_471759482$
10°	1.50	$-0.0_446237288$	$0.0_436844300$	$-0.0_59392988$	$-0.0_475638407$
10°	2.00	$-0.0_465549039$	$0.0_310559920$	$+0.0_44005017$	$-0.0_482850752$
10°	2.50	$-0.0_497574844$	$0.0_322853051$	$+0.0_31309557$	$-0.0_490740493$
10°	3.00	$-0.0_311255062$	$0.0_340845174$	$+0.0_32028169$	$-0.0_498491876$
5°	1.00	$-0.0_439567288$	$0.0_416135878$	$-0.0_42343141$	$-0.0_471759482$
5°	1.50	$-0.0_452970601$	$0.0_457750577$	$+0.0_54779976$	$-0.0_479554244$
5°	2.00	$-0.0_491778512$	$0.0_319591680$	$+0.0_31041383$	$-0.0_494047739$
5°	2.50	$-0.0_315613653$	$0.0_344295501$	$0.0_32868185$	$-0.0_310990270$
5°	3.00	$-0.0_324654228$	$0.0_380451766$	$0.0_35579754$	$-0.0_312548433$

Note: 0.0_36 means 0.0006

TABLE V

Final Results from All Data Calculated

Based on $\theta_1 = 25°$, $\gamma = 1.4$, $L = r_{pl}*$, $\dfrac{x}{L} = 0$ at $M = 0.001$

and $\Delta = \sqrt{\dfrac{\mathcal{D}_0 \, \lambda \, \sin \theta_2 \, (1 - \cos \theta_1)}{2\alpha_0 \, R_{min} \, (1 - \cos \theta_2)}}$

$\dfrac{T}{T_o}$	θ_2 °	M_{SA}	Δ	$\dfrac{T_{o_2}}{T_{o_1}}$	M_{actual}	Eff_{na}
1.0	15	1.5	$0.0_4 78115$		1.499931	0.9999827
		2.0			1.999965	0.9999806
		2.5			2.499934	0.9999765
		3.0			2.999887	0.9999731
	10	1.5			1.499975	0.9999772
		2.0			7.999951	0.9999728
		2.5			2.499907	0.9999669
		3.0			2.999831	0.9999598
	5	1.5			1.499961	0.9999641
		2.0			1.999908	0.9999489
		2.5			2.499814	0.9999339
		3.0			2.999668	0.9999209
0.6	15	1.5	$0.0_4 88026$	.99999026	1.499990	0.9999811
		2.0		.99998963	1.999978	0.9999774
		2.5		.99998895	2.4999505	0.9999713
		3.0		.99998828	2.9999137	0.9999676
	10	1.5		.99999009	1.499989	0.9999900
		2.0		.99998914	1.999967	0.9999708
		2.5		.99998811	2.499930	0.9999632
		3.0		.99998709	2.999871	0.9999563
	5	1.5		.99998957	1.499977	0.9999684
		2.0		.99998767	1.999933	0.9999504
		2.5		.99998559	2.499858	0.9999351
		3.0		.99998355	2.999741	0.9999219
0.2	15	1.5	$0.0_3 10718$	.99997770	1.5000074	0.9999845
		2.0		.99997627	1.999993	0.9999724
		2.5		.99997471	2.499973	0.9999651
		3.0		.99997317	2.999947	0.9999606

TABLE V (cont.) 73.

$\dfrac{T}{T_o}$	θ_2 °	M_{SA}	Δ	$\dfrac{T_{o2}}{T_{o1}}$	M_{actual}	Eff_{na}
	10	1.5		.99997731	1.500005	0.9999819
		2.0		.99997515	1.999986	0.9999674
		2.5		.99997278	2.499957	0.9999575
		3.0		.99997045	2.999935	0.9999550
	5	1.5		.99997613	1.499999	0.9999750
		2.0		.99997179	1.999963	0.9999512
		2.5		.99996703	2.499911	0.9999354
		3.0		.99996235	2.999824	0.9999204
1.0	15	1.5	$0.0_3 26704$	1.00000000	1.4999330	0.9999384
		2.0			1.999882	0.999934
		2.5			2.499780	0.999922
		3.0			2.9996213	0.9999098
	10	1.5			1.499916	0.9999228
		2.0			1.999834	0.9999078
		2.5			2.499683	0.9998873
		3.0			2.999438	0.9998593
	5	1.5			1.499869	0.9998795
		2.0			1.999690	0.9998278
		2.5			2.499378	0.9997788
		3.0			2.9988985	0.9997377
0.6	15	1.5	$0.0_3 29341$	0.99996753	1.499974	0.9999436
		2.0		0.999965442	1.999926	0.9999243
		2.5		0.99996316	2.499840	0.9999063
		3.0		0.999960922	2.9997015	0.9998899
	10	1.5		0.99996695	1.499961	0.9999310
		2.0		0.999963881	1.999888	0.9999017
		2.5		0.99996035	2.499766	0.9998771
		3.0		0.999956967	2.999570	0.9998546
	5	1.5		0.99996524	1.499924	0.9998954
		2.0		0.999958909	1.999775	0.9998340
		2.5		0.99995198	2.499527	0.9997838
		3.0		0.999945174	2.9991375	0.9997398
0.2	15	1.5	$0.0_3 35725$	0.99992568	1.500025	0.9999487
		2.0		0.999920908	1.999982	0.9999109
		2.5		0.99991569	2.499912	0.9998844
		3.0		0.99991052	2.9998236	0.9998686
	10	1.5		0.99992437	1.500016	0.9999391
		2.0		0.99917152	1.999952	0.9998905
		2.5		0.99990927	2.499866	0.9998616
		3.0		0.999901512	2.999787	0.9998508
	5	1.5		0.99992045	1.499993	0.9999140
		2.0		0.999905966	1.999874	0.9998350
		2.5		0.99989010	2.499695	0.9997817
		3.0		0.999874523	2.999414	0.9997350

TABLE V (cont.) 74.

$\dfrac{T}{T_o}$	$\theta_2{}^{o}$	M_{SA}	Δ	$\dfrac{T_{O2}}{T_{O1}}$	M_{actual}	Eff_{na}
1.0	15	1.5	0.0_378811		1.499796	0.9998124
		2.0			1.999648	0.9998044
		2.5			2.499375	0.9997777
		3.0			2.998864	0.9997294
	10	1.5			1.499745	0.9997655
		2.0			1.999502	0.9997233
		2.5			2.499037	0.9996575
		3.0			2.998316	0.9995989
	5	1.5			1.499708	0.9997315
		2.0			1.999076	0.9994866
		2.5			2.498139	0.9993380
		3.0			2.996684	0.9992098
0.6	15	1.5	0.0_388026	.99990259	1.499893	0.9998042
		2.0		.99989632	1.999783	0.9997758
		2.5		.99988949	2.499567	0.9997355
		3.0		.99988277	2.999145	0.9996792
	10	1.5		.99990087	1.499883	0.9997933
		2.0		.99989141	1.999663	0.9997042
		2.5		.99988107	2.499290	0.9996286
		3.0		.99987091	2.998710	0.9995637
	5	1.5		.99989573	1.49977	0.9996843
		2.0		.99987674	1.999328	0.9995034
		2.5		.99985596	2.498574	0.9993488
		3.0		.99983555	2.997415	0.9992198
0.2	15	1.5	0.0_210717	.99977705	1.500074	0.9998451
		2.0		.99976274	1.999934	0.9997261
		2.5		.99974709	2.499745	0.9996564
		3.0		.99973171	2.999471	0.9996058
	10	1.5		.99977311	1.500049	0.9998182
		2.0		.99975148	1.999856	0.9996715
		2.5		.99972781	2.499580	0.9995785
		3.0		.99970457	2.999361	0.99955245
	5	1.5		.99976137	1.499976	0.9997393
		2.0		.99971790	1.999625	0.9995096
		2.5		.99967035	2.499079	0.9993429
		3.0		.99962362	2.998242	0.999205
1.0	15	1.5	0.0_216615	1.00000000	1.499570	0.9996046
		2.0			1.999221	0.9995838
		2.5			2.498612	0.9995063
		3.0			2.997605	0.9994294
	10	1.5			1.499470	0.9995080
		2.0			1.998885	0.9993804
		2.5			2.497965	0.9992761
		3.0			2.996450	0.9991540

TABLE V (cont.)   75.

$\dfrac{T}{T_o}$	θ_2 o	M_{SA}	Δ	$\dfrac{T_{o2}}{T_{o1}}$	M_{actual}	Eff_{na}
1.0	15	1.5	0.0_216615	1.00000000	1.499570	0.9996046
		2.0			1.999251	0.9995838
		2.5			2.498612	0.9995063
		3.0			2.997605	0.9994294
	10	1.5			1.499470	0.9995080
		2.0			1.998885	0.9993804
		2.5			2.497965	0.9992761
		3.0			2.996450	0.9991540
	5	1.5			1.49932	0.9993747
		2.0			1.998053	0.9989179
		2.5			2.496068	0.9986006
		3.0			2.993009	0.9983324
0.6	15	1.5	0.0_218557	0.00079464	1.499832	0.9996402
		2.0		0.99978146	1.999529	0.9995198
		2.5		0.00076704	2.499005	0.9994133
		3.0		0.99975287	2.998199	0.9993240
	10	1.5		0.99979101	1.49975	0.9995612
		2.0		0.99977108	1.999290	0.9993767
		2.5		0.99974929	2.498502	0.9992166
		3.0		0.99972787	2.997281	0.9990802
	5	1.5		0.99978019	1.499524	0.9993426
		2.0		0.99974015	1.998587	0.9989551
		2.5		0.99969635	2.496998	0.9985858
		3.0		0.99965330	2.994546	0.9983533
0.2	15	1.5	0.0_222594	0.99953004	1.500059	0.9995843
		2.0		0.99949987	1.999859	0.9994216
		2.5		0.99946690	2.499468	0.9992778
		3.0		0.9994344	2.998886	0.9991692
	10	1.5		0.99952173	1.5000181	0.9995384
		2.0		0.99947614	1.999696	0.9993073
		2.5		0.99942627	2.499112	0.9991107
		3.0		0.99937728	2.998653	0.9990567
	5	1.5		0.99949698	1.499948	0.9994492
		2.0		0.99940537	1.999208	0.9989656
		2.5		0.99930516	2.498060	0.9986155
		3.0		0.99920668	2.996309	0.9983277

LIST OF REFERENCES

1. Backer, G. H. Design and Performance of an Adjustable Two-Dimensional Nozzle with Boundary Layer Correction. Jour. Aero. Sci., 21:1, pp. 50-56, 1954.

2. Brinich, Paul. Boundary Layer Measurements in a 3.84 by 10-Inch Supersonic Channel. NACA TN 2203, 1950.

3. Carrier, George. Foundations of High Speed Aerodynamics. New York: Dover Publications, Inc., 1951.

4. Cohen, Clarence and Eli Reshotko. Similar Solutions for the Compressible Laminar Boundary Layer with Heat Transfer and Pressure Gradient. NACA Report 1293, 1956.

5. Chapman, Dean and M. Rubesin. Temperature and Velocity Profiles in the Compressible Laminar Boundary Layer with Arbitrary Distribution of Surface Temperature. Jour. Aero. Sci., 16:9, pp. 547-565, 1949.

6. Durand, W. F. Aerodynamic Theory, Vols. I and III. California: Durand Reprinting Committee, California Institute of Technology, 1943.

7. Gazley, Carl. Boundary Layer Stability and Transition in Subsonic and Supersonic Flow. Jour. Aero. Sci., 20:1, 19-28, 1953.

8. Goldstein, S. Modern Developments in Fluid Dynamics, Vols. I and II. First Ed., London: Oxford University Press

9. Lighthill, M. J. Methods of Predicting Phenomena in High Speed Flow of Gases. Jour. Aero. Sci., 16:2, pp. 69-83, 1949.

10. Low, George. Simplified Method for Calculation of Compressible Laminar Boundary Layer with Arbitrary Free-Stream Pressure Gradient. NACA TN 2531, 1951.

11. McLellan, C., T. Williams, and I. Beckwith. Investigation of the Flow Through a Single Stage Two Dimensional Nozzle in the Langley Eleven Inch Hypersonic Tunnel. NACA TN 2223, 1950.

12. Oswatitsch, Klaus. Translated by Gustav Kuerti. Gas Dynamics. First Ed., New York: Academic Press, Inc., 1956.

13. Pai, Shih-I. _Viscous Flow Theory, I-Laminar Flow._ First Ed., New York: D. Van Nostrand Company, Inc., 1956.

14. Sauer, Robert. Translated by F. K. Hill and R. A. Alpher. _Introduction to Theoretical Gas Dynamics._ Ann Arbor: J. W. Edwards, 1947.

15. Schaaf, S. A. An Axially-Symmetric Nozzle with Boundary Layer Correction. University of California Eng. Proj. Report HE-150-58, June 15, 1949.

16. Schlichting, Hermann. Translated by J. Kestin. _Boundary Layer Theory._ New York: McGraw-Hill Book Co., Inc., 1955.

17. Shapiro, Ascher. _The Dynamics and Thermodynamics of Compressible Fluid Flow, Vols. I and II._ First Ed., New York: The Ronald Press Company, 1953.